Spectroscopic Approach for Identification of Key Factors and Elucidation of Mechanism of Drug Dissolution from Orally Administered Solid Dosage Forms

著者	有安 葵
著者（英）	Ariyasu Aoi
学位名	博士（薬科学）
学位授与機関	武蔵野大学
学位授与年度	2017年度
学位授与番号	32680甲第39号
URL	http://id.nii.ac.jp/1419/00000834/

Doctoral Dissertation

Spectroscopic Approach for Identification of Key Factors and Elucidation of Mechanism of Drug Dissolution from Orally Administered Solid Dosage Forms

Aoi Ariyasu

Graduate School of Pharmaceutical Sciences
Musashino University

FY2017

Contents

Introduction....2

Study 1: Delay effect of magnesium stearate on tablet dissolution in acidic medium....5

1. Background....5

2. Materials and methods....5

3. Results and Discussion....9

4. Conclusion....20

Study 2: Non-destructive Prediction of Enteric Coating Layer Thickness and Drug Dissolution Rate by Near-infrared spectroscopy and X-ray computed tomography....21

1. Background....21

2. Materials and methods....22

3. Results and Discussion....25

4. Conclusion....35

Overall Conclusion....37

References....39

List of Publications....44

Acknowledgement....45

Introduction

The dissolution of orally administered solid dosage forms is a critical quality aspect, that can affect the bioavailability and pharmacokinetic (PK) profile, and eventually, the efficacy and safety of the drug products [1]. After a drug product is orally administered, the drug substance undergoes dissolution, membrane permeation, distribution, metabolism, and excretion *in vivo* (Figure 1). While the behavior of a drug substance during processes occurring after membrane permeation depends on the type of the drug substance, the dissolution process can be controlled by the drug product independently of the drug substance. Thus, the control of *in vivo* dissolution can contribute to control of the PK profile through the control of absorption. Many attempts have been made to control *in vivo* dissolution, and many types of controlled-release drug products have been developed to achieve the expected *in vivo* dissolution in the gastrointestinal tract and yield PK profiles different from those obtained with general immediate-release drug products. Enteric drug products are designed not to dissolve in stomach and dissolve in intestine. Extended-release drug products are designed to dissolve slowly for a few hours or more. To achieve such unusual dissolution, controlled-release drug products tend to have the complex formulation and/or complicated dissolution mechanism. The need to develop such difficult pharmaceutical product is increasing in the pharmaceutical industry.

Drug dissolution from drug products depends not only on the dissolution properties of the drug itself but also on the formulation (excipients and composition) and the manufacturing process of the drug product, as well as the properties of the medium in which the drug is dissolved, such as the pH, salt, and surfactant concentration [2]. Since many factors contribute to drug dissolution from the drug product, the dissolution process is very complex, leading to difficulties in controlling the process. Therefore, for pharmaceutical product development and quality control of orally administered drug products, it is essential to understand the dissolution mechanism and identify the key factors affecting the dissolution properties to control them properly.

Among analytical techniques, spectroscopic techniques such as infrared (IR), near-IR (NIR), Raman, and X-ray spectroscopy are extremely powerful tools for evaluation of drug products because of their ability to provide quick and nondestructive measurements [3]. In addition, a single spectrum obtained by one-time measurements using a spectroscopic technique contains a large amount of information. Depending on the type of technique used, the spectrum can contain information regarding the molecule structure, crystal structure, component composition, and/or other physicochemical properties of the target material [3]. These characteristics of spectroscopic techniques enable nondestructive prediction of the physicochemical properties of the drug product or real-time monitoring of its dynamic physicochemical properties, including dissolution. Actually, these techniques are used as process analytical technology (PAT) tools for real-time monitoring of the manufacturing process and applied for real-time release (RRT) testing [4].

Given both the complex nature of drug product dissolution and characteristics of spectroscopic techniques, it was deemed appropriate that spectroscopic techniques be applied for identification of the key factors and elucidation of the mechanism of drug dissolution from orally administered solid dosage forms. Although there are many types of orally administered drug products and multiple types of dissolutions, two topics were selected for research in this doctoral dissertation: (1) the delay effect of magnesium stearate on tablet dissolution in an acidic medium and (2) non-destructive prediction of enteric coating layer thickness and drug dissolution rate by near-infrared spectroscopy (NIRS) and X-ray computed tomography (CT). In the assessment of each of these topics, different spectroscopic techniques were applied to different targets and for different purposes. In the former case, scanning electron microscopy-energy dispersion spectroscopy (SEM-EDS) and attenuated total reflection-Fourier transform infrared spectroscopy (ATR-FTIR) were used to elucidate the dissolution-retardation mechanism mediated by magnesium stearate (Mg-St) in immediate-release tablets: in the latter case, NIRS and X-ray CT were used to identify the key factors that determine the dissolution rate of enteric-coated tablets.

Spectroscopic techniques have many advantages like quick and nondestructive measurements, and large amount and detailed information available. One type of spectroscopic techniques like FTIR and NIRS enables monitoring of the chemical change of the target material at a molecular level, and another type like SEM and X-ray CT enables micro-level spatial analysis of targets. On the other hand, they often require analysis/processing techniques to extract the target information from the spectrum data. One spectrum contains a large amount of information incorporating the spectra derived from multiple sources and does not present a specific result. Thus, analysts must analyze the spectrum to understand what each peak represents and process the spectrum to extract the information they need by using general databases or comparing the findings with results obtained by other techniques. Therefore, it is also important to establish the analysis/processing procedures for spectroscopic techniques. In this regard, the purpose of my research is to establish some spectroscopic approaches for identification of key factors and elucidation of the mechanism of drug dissolution from orally administered solid dosage forms from an analytical scientist's perspective. If these approaches are established, they would facilitate pharmaceutical product development, which has become increasingly complicated, and eventually allow advancement of research in the area of formulation development.

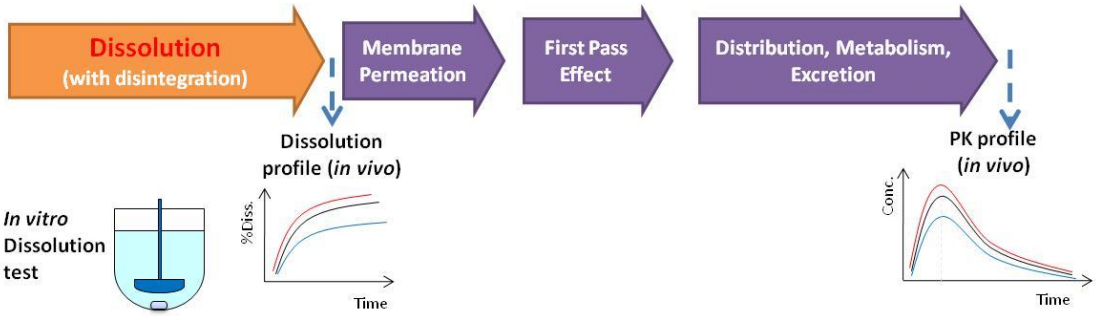

Figure 1 Illustration of *in vivo* behavior of drug substance from orally administered drug product

Study 1: Delay effect of magnesium stearate on tablet dissolution in acidic medium

1. Background

Magnesium stearate (Mg-St) is a traditional and commonly used lubricant for solid dosage formulations [5], and is also known to delay tablet dissolution because of its hydrophobicity [6]. Although there have been many studies investigating the mechanism of action and characteristics of Mg-St [7–9], there is still room for investigation, and some problems related to Mg-St are still being reported, for example, the decrease of tablet hardness, sticking trouble, and over lubrication by over mixing [10–13], which sometimes induces the delay of tablet disintegration/dissolution [14,15].

When *in vitro* dissolution tests were conducted for one brand of marketed metformin HCl 500 mg tablets, dissolution profiles varied depending on the pH of the medium, in spite of the constant high solubility of metformin HCl being independent of pH. Because components other than Mg-St in the tablet formulation were soluble, the properties of Mg-St were briefly investigated. The different properties of Mg-St in media of different pH and the correlation between Mg-St dispersibility and dissolution rate of the tested tablet was suggested, and thus, these properties were investigated in this study using commercial metformin HCl tablets and prepared model metformin HCl tablets.

There have been many studies which conducted the comparison of the disintegration and dissolution of tablets containing different kinds of lubricant [16–18], different kinds or amounts of Mg-St [19,20], or tablets manufactured with the same formulation but different process parameters. However, few studies have examined the drug dissolution mechanism from tablet containing Mg-St. In this study, the mechanism of action by which Mg-St delays tablet dissolution was investigated using spectroscopic techniques, and the behavior of Mg-St was examined in acidic and neutral pH conditions reflecting stomach and intestinal pH environment.

2. Materials and methods

2.1 Materials

2.1.1. Materials

Three commercial metformin HCl 500 mg tablets were purchased and used for dissolution tests.

For preparation of model tablets, metformin HCl was purchased from Farmhispania S.A. (Barcelona, Spain), which meets the specifications in Japanese Pharmacopoeia (JP), European Pharmacopoeia (Ph.Eur.), and the U.S. Pharmacopeia (USP). Its crystal form was the known thermodynamically stable form. Povidone (polyvinylpyrrolidone) was purchased from BASF (Ludwigshafen, Germany), Mg-St was purchased from Wako Pure Chemical Industries, Ltd. (Tokyo, Japan), and they were used for preparation of model tablets.

Stearic acid (>98.0%) and Mg-St purchased from Tokyo Chemical Industry Co., Ltd. (Tokyo, Japan) were used for obtaining reference IR spectra.

2.1.2. Preparation of model tablets

To prepare wet granules, 9.5 g of metformin HCl and 0.5 g of povidone were mixed in a mortar with the gradual addition of 1.5 mL of water. Then, extruding granulation was carried out using an 850-μm screen, and the wet granules were dried for 1 day at 70ºC. The subsequent granules were compressed with a compression testing machine (TG-50KN, Minebea Co., Ltd., Nagano, Japan) with a diameter of 8 mm. The 200 mg tablets were prepared with a compression speed of 10 mm/min and a pressure of 13 kN, without Mg-St ("Mg-St(-)" tablets).

The tablets containing 1% Mg-St ("Mg-St(+)" tablets) were prepared by adding 1% (w/w) Mg-St to the dried granules. The granules were mixed for 1 min and compressed under the same conditions as the "Mg-St(-)" tablets.

2.1.3. Preparation of dissolution medium

For the dissolution tests of commercial metformin HCl tablets, the recommended dissolution media described in Ph.Eur. were used: simulated gastric fluid without pepsin (SGF, c.a. pH 1.2), acetate buffer (c.a. pH 4.5), and phosphate buffer (c.a. pH 6.8).

For the other experiments, the 1st and 2nd fluid for dissolution test, described in JP, were used ("pH 1.2" and "pH 6.8", respectively). pH 1.2 and pH 6.8 media containing 0.01% (w/v) $MgSO_4$ were also used ("pH 1.2 (Mg+)" and "pH 6.8 (Mg+)", respectively).

2.2 Methods

2.2.1. Dissolution tests

A dissolution test apparatus (Evolution 6100, Distek, Inc., New Jersey) was used. The medium volume was 900 mL controlled at 37.2±0.5ºC during the test, and the basket rotation speed was 100 rpm. Dissolution tests were conducted according to harmonized procedure within JP, Ph. Eur., and USP. The medium was removed at each time point and its drug concentration was analyzed by HPLC analysis.

An appropriate HPLC apparatus with UV detection unit for the determination purpose was used. The determination method by HPLC was validated one, and the HPLC operating conditions were as follows: the analytical column was C8 column, and the mobile phase was a mixture of aqueous solution, acetonitrile and sodium dodecyl phosphate, UV detection wavelength was 265 nm, and the isocratic programs was applied.

2.2.2. Initial dissolution rate measurement

The drug release rate from the tablet depends on not only the dissolution speed of components but also the tablet disintegration behavior, because changes in exposed surface area to the dissolution medium can influence the drug release rate. The stationary disk method is useful for examining the intrinsic drug release rate from tablet components keeping tablet surface area constant at the initial stage of dissolution studies while eliminating the drug size effect [21]. In this study, the tablet holder was used for the stationary disk method. The test tablet was placed into the holder to expose the single face (circle with 6 mm diameter) to the test solution and was suspended in the dissolution medium over the paddle as shown in Figure 2. The tablet was set so that its diametrical direction could be in line with the water flow.

A dissolution test apparatus (NTR-3000, Toyama Sangyo Co., Ltd., Toyama, Japan) and fiber multi-channel spectrometer (S-2450, Soma Optics, Ltd., Tokyo) were used. The medium volume was 900 mL, controlled at 37.2±0.5ºC during the test, and the paddle rotation speed was 50 rpm. The probe of the spectrometer was dipped in the dissolution vessel and UV spectra of the medium were monitored during the dissolution tests with the following conditions: exposure time was 20 ms, light path length was 5 mm, measurement interval was 5 s, and cumulated number was 50. The detection wavelength was set at 235 nm for pH 1.2 medium and 245 nm for pH 6.8 medium in consideration of different UV spectrum pattern of metformin in both media.

2.2.3. Elemental mapping of Mg on tablet surface by SEM-EDS

The distributions of Mg on the tablet surface before and during the dissolution test were observed under a scanning electron microscope (SEM, JSM-7600F, JEOL, Tokyo) with an energy dispersive X-ray spectrometer (EDS, JED-3200 Series, JEOL). The testing tablet was taken out from the medium after 5 min of dissolution according to the procedures in 2.2.2 and dried. The acceleration voltage was 15 kV, magnification ratio was x100, and measurement time was 10 h for the detection of Mg.

2.2.4. ATR-FTIR analysis

A Fourier transform infrared spectroscopy (FTIR) apparatus (Spectrum One, Perkin Elmer, Massachusetts) was used for the surface measurement of the tablet. The scan range was 4000 – 400 cm^{-1}, resolution was 4 cm^{-1}, and scan number was 4. Using attenuated total reflection (ATR) mode, where crystal material was diamond/KRS-5 and incident angle for the sample was about 45º, IR spectra of the tablet surface were obtained before and after 2 min of the dissolution studies of basket 100 rpm according to the procedures in 2.2.1.

FTIR apparatus (IRTracer-100, Shimazu, Kyoto, Japan) was used to obtain the reference IR spectra of stearic acid and Mg-St. The measurement parameters used were the same as above. The spectra of Mg-St exposed to the media overnight were also obtained.

5. Noyes-Whitney equation

The drug dissolution rate can be represented by the Noyes-Whitney equation [22]:

$$dC/dt = kS(C_S - C) \quad (1)$$

where C_S is the solubility of the drug or the concentration of its saturated solution, C is the concentration of the dissolved drug at time t, S is the exposed surface area of the drug, and k is a constant specific to the drug.

When C_S is much larger than C (for example, at the initial stage of dissolution), the equation can become:

$$dC/dt = kSC_S \quad (2)$$

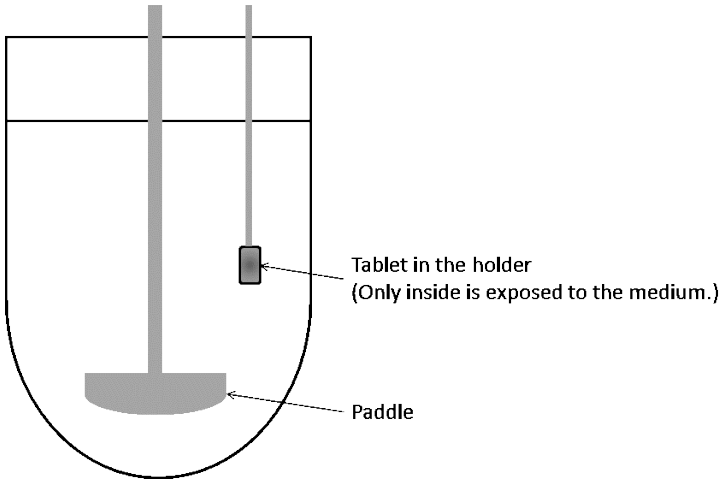

Figure 2 Diagram of stationary disk method.

3. Results and Discussion

3.1. pH dependence of dissolution profiles of commercial metformin HCl tablets

To investigate the pH dependency of dissolution profiles of metformin HCl tablets, *in vitro* dissolution tests were conducted for three different metformin HCl 500 mg tablets marketed in different countries. Dissolution tests were done according to the test conditions described in the guideline (EMEA, 2010); the apparatus used was basket at 100 rpm and the dissolution medium was simulated gastric fluid without pepsin (SGF, c.a. pH 1.2), acetate buffer (c.a. pH 4.5), and phosphate buffer (c.a. pH 6.8). The obtained dissolution profiles are shown in Figure 3. All three kinds of tablets showed the same rank order of dissolution rate (pH 1.2 = pH 4.5 < pH 6.8) and the same dissolution process where the drug dissolution occurred on the tablet surface without disintegration.

Metformin HCl is a biguanide widely used for the treatment of type 2 diabetes mellitus [24]. The properties of metformin HCl is summarized in the review article [25]. The data in Japanese orange book shows that its aqueous solubility is consistently high in the physiological pH range and is independent of pH (333 mg/mL in pH 1.2, 353 mg/mL in pH 4.0, 355 mg/mL in pH 6.8 and 346 mg/mL in water at 37ºC), and its pKa is 12.4. This constantly high solubility satisfied the sink condition for the dissolution tests, as shown in Figure 3; the solubility was more than one-hundred times the sink condition in every medium (against the maximum possible metformin concentration of 0.56 mg/mL = 500 mg/900 mL). Therefore, the difference in the drug dissolution rate in different pH media observed was not expected to be caused by the properties of metformin HCl itself. While every formulation tested was composed of metformin HCl, povidone, Mg-St, and hypromellose, the composition differed slightly between formulations based on slightly different tablet weight. Both povidone and hypromellose are water-soluble compounds, and only Mg-St is poorly soluble.

When Mg-St was added to these media, it tended to float on the surface of medium of pH 1.2 or pH 4.5 buffer. However, it dispersed in the pH 6.8 buffer. This varying tendency of Mg-St dispersibility could explain the observed tablet dissolution rate order of pH 1.2 = pH 4.5 < pH 6.8. Based on these observations, it was suggested that the difference in dissolution rate of these metformin HCl tablets in different pH media could be attributed to the properties of Mg-St.

In the following experiments, prepared model metformin HCl tablets were used to investigate the behavior of Mg-St contained in tablets, and JP 1st and 2nd fluid for dissolution test (pH 1.2 and pH 6.8 media) were applied to investigate the dissolution behaviors of Mg-St and the tablets in acidic and neutral media.

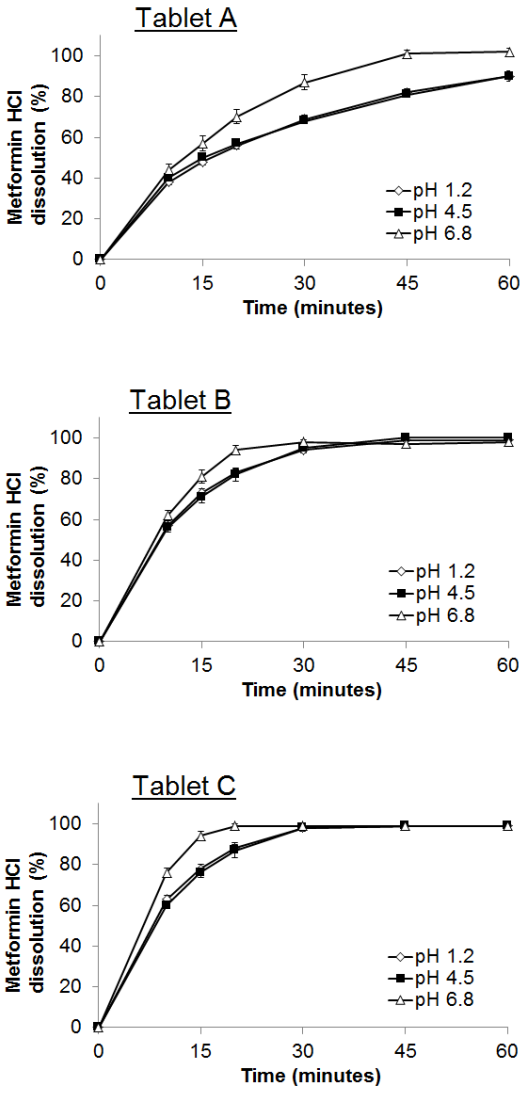

Figure 3 Dissolution profiles in different pH media of metformin HCl 500 mg tablets marketed in different countries. Each dissolution profile is the average ± SD bar for all time points (n=12 each).

3.2. Retardation of drug dissolution from tablets containing Mg-St

The dissolution rate of tablets depends on not only the physicochemical properties of the tablet components, such as solubility and diffusion coefficient, but also their exposed surface area to the dissolution medium [26], often expressed by the Noyes-Whitney equation (Eq. (1)). In the case of model metformin HCl 200 mg tablets, this equation can be simplified to Eq.2, because the solubility of metformin HCl (C_S) is more than one-thousand times the sink condition against the possible maximum concentration of metformin in the vessel of 0.22 mg/mL = 200 mg/900 mL.

Through the course of dissolution studies, the surface area of tablets can change. For example, in

the case of non-disintegrating tablets, surface area decreases with a decrease in tablet size along with dissolution, and in the case of disintegrating tablets, surface area increases as tablets disintegrate to granules. The dissolution mechanism of both commercial metformin HCl 500 mg tablets and model metformin HCl 200 mg tablets was surface dissolution-limited dissolution without disintegration. To eliminate the influence of surface area decrease and investigate the intrinsic dissolution from the given surface area, the initial drug dissolution rates of prepared model tablets were measured by the stationary disk method by using both pH 1.2 and pH 6.8 media. The resulting dissolution profiles are shown in Figure 4. In both media, Mg-St(+) tablets showed slower drug dissolution than Mg-St(-) tablets because of the hydrophobic property of Mg-St, in spite of the very high solubility of metformin HCl. A larger retardation effect of Mg-St was observed in pH 1.2 medium than in pH 6.8 medium; this is discussed later in this paper, and the common mechanism of dissolution retardation in both media by Mg-St is discussed in the following part.

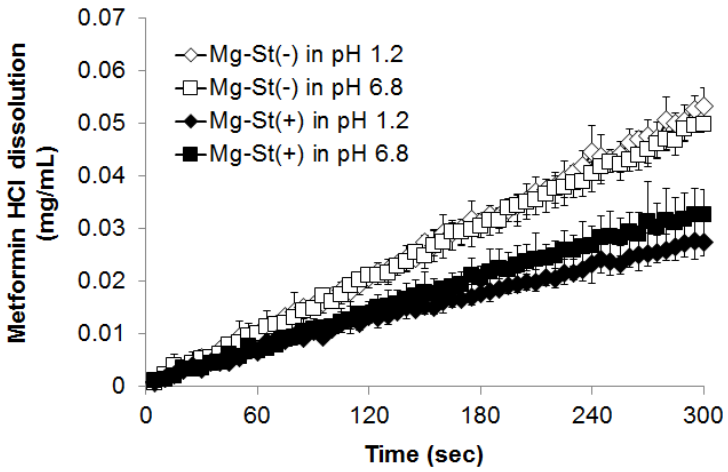

Figure 4 Initial dissolution rate profiles of Mg-St(-) tablets and Mg-St(+) tablets in pH 1.2 and pH 6.8 media by stationary disk method. Each profile is the average with maximum-minimum bar for all time points (n=3 each).

3.3. Limitation of tablet dissolution by Mg-St dissolution

Because the presence of Mg-St in tablets caused the delay of drug dissolution, it was suggested that the dissolution of Mg-St itself was controlling the dissolution of these tablets. Mg-St is a poorly water-soluble compound; its solubility in water is 4 mg/100 mL at 25ºC. Therefore, the solubility product of Mg-St should be taken into account for the dissociation of Mg-St into Mg^{2+} ions and stearic acid ions in the region near the tablet surface. If the dissolution medium is saturated by Mg^{2+} ions, the dissociation and dissolution of Mg-St are inhibited.

To investigate the effect of Mg-St dissolution on the tablet dissolution, the dissolution studies were performed with media containing 0.01% $MgSO_4$ (w/v), which corresponds to about 1 mmol/L Mg^{2+} ions. The resulting dissolution rate profiles are shown in Figure 5.

Then, the initial dissolution rate was calculated based on profiles in Figure 4 and Figure 5. The profiles showed that the drug dissolution rate of Mg-St(-) tablets was almost constant for the tested 5 min; thus, the dissolution rate for Mg-St(-) tablets was calculated based on the profiles obtained during the initial 5 min. In contrast, the dissolution rates for Mg-St(+) tablets appeared to decrease in the later stage of dissolution. For Mg-St(+) tablets, dissolution rates in the initial 2 min and between 2 and 5 min were calculated separately, and the dissolution rates during 2 to 5 minutes were used for the subsequent evaluation. The obtained dissolution rates are listed in Table 1.

The ratio of the dissolution rate in medium with $MgSO_4$ to that in medium without $MgSO_4$ was calculated for each tablet and in each pH medium. The ratios of Mg-St(-) and Mg-St(+) tablets in pH 1.2 media were 0.97 and 0.81, respectively, and those in pH 6.8 media were 0.92 and 0.76, respectively. The ratios of Mg-St(-) tablets in both media were almost 1, indicating that the existence of Mg^{2+} ions had little influence on the dissolution of Mg-St(-) tablets. The ratios of Mg-St(+) tablets were less than those of Mg-St(-) tablets. These results indicated that the existence of Mg^{2+} ions delayed the dissolution of Mg-St(+) tablets, suggesting that the dissolution of Mg-St limits the tablet dissolution.

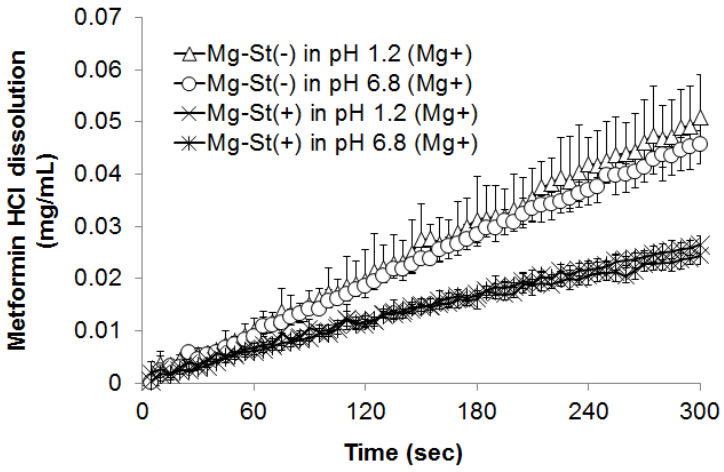

Figure 5 Initial dissolution profiles of Mg-St(-)and Mg-St(+) tablets in pH 1.2 and pH 6.8 media containing 0.01% $MgSO_4$ (w/v) by stationary disk method. Each profile is the average with maximum-minimum bar for all time points (n=3 each). pH 1.2 (Mg+): pH 1.2 medium containing 0.01% $MgSO_4$; pH 6.8 (Mg): pH 6.8 medium containing 0.01% $MgSO_4$.

3.4. Elemental mapping of Mg on the tablet surface

To investigate the surface state of Mg-St(+) tablets, Mg distribution on the Mg-St(+) tablet surface before and during the dissolution test was observed by Mg detection with SEM-EDS. This is a general method used to observe Mg on the sample surface [27]. The Mg maps are shown in Figure 6. Compared to the surface before the dissolution, the increased amount of Mg was detected after 5 min of dissolution in both pH 1.2 and pH 6.8 media; hence, the maps show undissolved and remaining Mg on the surface of Mg-St(+) tablets during dissolution.

Because the SEM-EDS observation of Mg-St was based on magnesium derived from Mg-St, determination of Mg-St on the tablet surface was performed based on the stearyl ($CH_3(CH_2)_{16}COO$-) or palmitic ($CH_3(CH_2)_{14}COO$-) base derived from Mg-St by measuring ATR-FTIR. The surfaces of Mg-St(-) tablets and Mg-St(+) tablets were analyzed by ATR-FTIR before and after 2 min of dissolution to detect any chemical change of tablet surface components. The FTIR spectra are shown in Figure 7. In any spectrum of Mg-St(+) tablets, two characteristic peaks at about 2920 and 2850 cm^{-1} were observed, which were not observed in the spectra of Mg-St(-) tablets. These peaks are derived from the aliphatic CH of the stearyl or palmitic base of Mg-St. Compared to the spectrum before dissolution, these peaks increased relatively after dissolution, which indicates the increase in the relative ratio of Mg-St on the tablet surface. These data also supported the increased amount of Mg-St exposed on the tablet surface after dissolution. Because of the slow dissolution rate of Mg-St, the amount of Mg remaining increased; therefore, the dissolution of Mg-St is the rate-limiting step of the tablet dissolution.

These observations of the relative increase of Mg-St on the Mg-St(+) tablet surface by dissolution are also consistent with the result that the initial dissolution rate of Mg-St(+) tablets decreases in the later stage of the profiles (2-5 min), as discussed in the results of initial dissolution rate. Along with the increase in the relative ratio of Mg-St on tablet surface by dissolution, the drug dissolution rate of Mg-St(+) tablets decreases more than the initial rate.

(a) pH 1.2

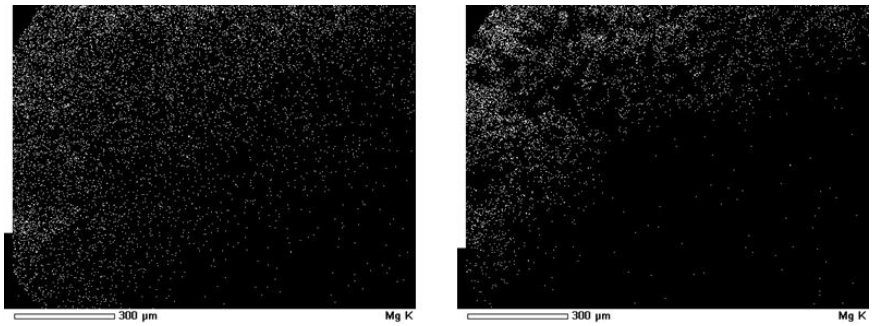

(b) pH 6.8

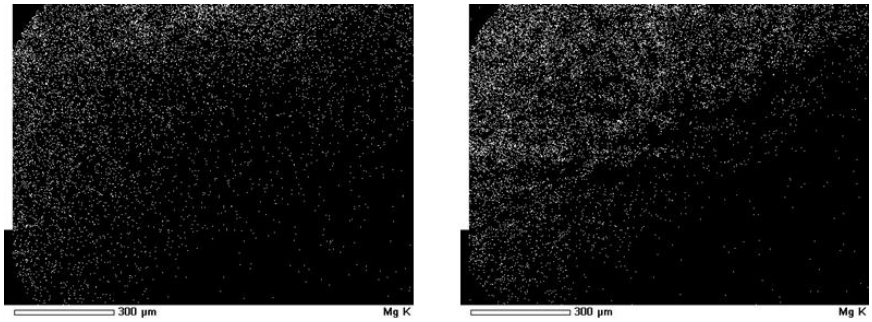

Figure 6 Mg detected by SEM-EDS on the surface of Mg-St(+) tablets before and after the dissolution for 5 minutes in pH 1.2 medium (a) and pH 6.8 medium (b). Left: surface before dissolution; Right: surface after dissolution for 5 minutes.

1) Before dissolution

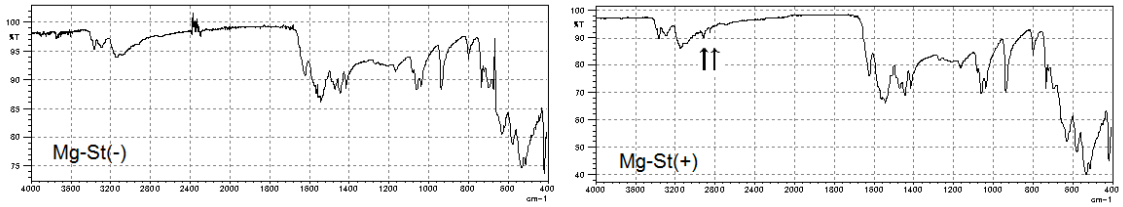

2) After 2 minutes dissolution in pH 1.2

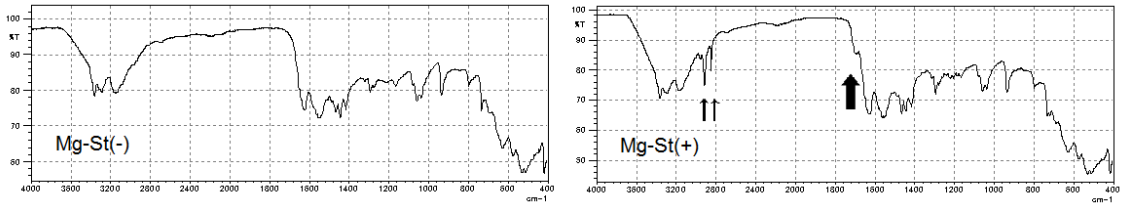

3) After 2 minutes dissolution in pH 6.8

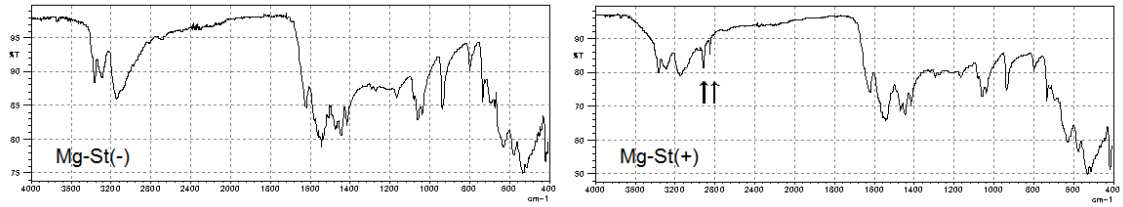

Figure 7 FTIR spectra of Mg-St (-) tablets and Mg-St(+) tablets before and after 2 minutes dissolution in pH 1.2 and pH 6.8 media. Left: Mg-St(-) tablets; right: Mg-St(+) tablets. Double arrow indicates the peaks of around 2920 and 2850 cm^{-1}. Black thick arrow indicates the peak around 1700 cm^{-1} derived from stearic acid.

3.5. Dependency of delay of tablet dissolution by Mg-St on dissolution medium pH

The delay of tablet dissolution by Mg-St was discussed in the previous part. Its different behaviors in different pH media are discussed in the following part.

When the initial dissolution rate of Mg-St(+) tablets in pH 1.2 medium was compared to that in pH 6.8 medium, as shown in Figure 4, the dissolution in pH 1.2 medium was found to be slower than in the pH 6.8 medium. Table 1 indicates that the drug dissolution rates decreased to 47% and 62%, in the media of pH 1.2 and 6.8 respectively, by adding Mg-St to the tablets. These findings suggested that the contributions of Mg-St to the delay might be larger in pH 1.2 medium than in pH 6.8 medium.

In Figure 7, Mg-St(+) tablets after 2 min of dissolution in pH 1.2 medium displayed one characteristic peak at around 1700 cm^{-1}. The region around this peak can be assigned to a carboxylic group. Figure 8 shows the IR spectra of stearic acid and Mg-St, obtained by the same procedure as that used for the measurement of tablets. Although major parts of both spectra were similar, the peak at around 1700 cm^{-1} was observed only for stearic acid, which is probably derived from carboxylic acid C=O. In addition, Mg-St was dispersed on the surface of pH 1.2 and pH 6.8 media overnight, and IR spectra of the Mg-St were obtained (Figure 8). The results showed that only Mg-St exposed to pH 1.2 medium presented the peak at 1700 cm^{-1}, suggesting the transformation to stearic acid. This peak was consistent with the peak observed for Mg-St(+) tablets after dissolution in pH 1.2 medium. Based on these results, it was suggested that the Mg-St on the tablet surface might dissociate to its ions and undergo hydrogenation to form stearic acid in pH 1.2 medium. Such changes can occur, as reported in a previous study [28], although their dissolution mechanism is different from the one in this study.

The solubility of stearic acid is 3 mg/L in water at 20ºC, which is approximately one-tenth of the solubility of Mg-St. Therefore, the generation of stearic acid on the tablet surface can cause the additional inhibition of tablet dissolution because of its low solubility in acidic medium. Considering the pKa of stearic acid (4.95), it is possible that a part of Mg-St near the tablet surface is firstly dissolved and immediately hydrogenated to stearic acid by exposure to pH 1.2 medium, which contributes to further delay of tablet dissolution. Although Mg-St contains not only magnesium stearate but also magnesium palmitate [29], the same behavior is assumed for magnesium palmitate since both substances are similar, with only difference in the carbon number. Palmitic acid shows a similar IR spectrum to stearic acid, with the characteristic peak at around 1700 cm^{-1}. The solubility of palmitic acid in water is as low as that of stearic acid, and this may cause the delay of tablet dissolution in the same way.

Table 1　Initial dissolution rates of Mg-St(-)and Mg-St(+) tablets

Dissolution rate in pH 1.2 medium [μg/mL/sec]

medium	Mg-St(-) tablets [μg/mL/sec]			Mg-St(+) tablets [μg/mL/sec]		
$MgSO_4$	0-2 min	2- 5 min	Total	0-2 min	2- 5 min	Ratio (+/-)
(-)	0.171	0.179	0.176	0.114	0.083	0.47
(+)	0.167	0.168	0.170	0.108	0.067	0.39
Ratio(+/-)			0.97		0.81	

Dissolution rate in pH 6.8 medium [μg/mL/sec]

medium	Mg-St(-) tablets [μg/mL/sec]			Mg-St(+) tablets [μg/mL/sec]		
$MgSO_4$	0-2 min	2- 5 min	Total	0-2 min	2- 5 min	Ratio (+/-)
(-)	0.171	0.163	0.169	0.119	0.104	0.62
(+)	0.155	0.150	0.155	0.101	0.079	0.51
Ratio(+/-)			0.92		0.76	

*Ratio was calculated with underlined results.

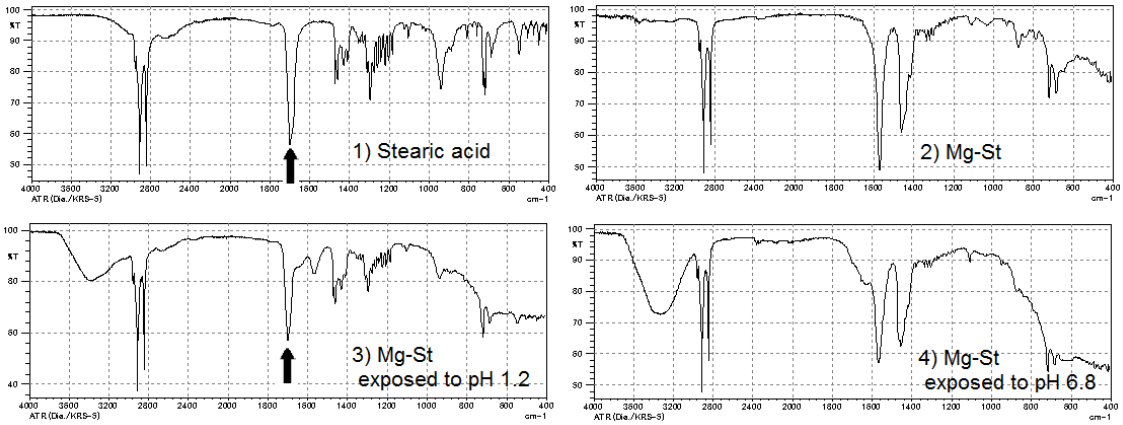

Figure 8　IR spectra of stearic acid and Mg-St measured by ATR-FTIR. 1) Stearic acid; 2) Mg-St; 3) Mg-St exposed to pH 1.2 medium; 4) Mg-St exposed to pH 6.8 medium. Black arrow indicates the peak at around 1700 cm^{-1} characteristic to stearic acid.

3.6. Delay mechanism of tablet dissolution by Mg-St in acidic and neutral media

Based on the investigation results and considerations in this study, the proposed inhibition mechanism of tablet dissolution by Mg-St is shown in Figure 9.

When the Mg-St(+) tablet is exposed to the dissolution medium, metformin HCl granules dissolve faster than Mg-St, because Mg-St is less soluble in water than both metformin HCl and povidone. As a result, the area covered by Mg-St increases (Step 1), as confirmed by SEM-EDS and ATR-FTIR studies, and effective surface area, reported by Sekiguchi et al [21], decreases. The effective drug surface area can be discussed by the results of initial dissolution rates with the stationary disk method as follows. The results of the initial dissolution rate measurement correspond to kSC_S in Eq. (2), and k and C_S depend on the combination of drug and dissolution medium. Therefore, the ratio of the initial dissolution rate represents the ratio of S (exposed surface area of the drug) of Mg-St(+) tablets to S of Mg-St(-) tablets in each medium. In the pH 6.8 medium, the ratio was 0.62, indicating 38% of the drug surface was covered by Mg-St and thus the effective surface area was decreased by 38%.

The dissolution of Mg-St limits the tablet dissolution (Step 2), as shown in the dissolution studies with Mg^{2+} ions added. The Mg-St(+) tablet dissolution rate decreased in the conditions under which the dissociation and dissolution of Mg-St were inhibited. In the case of dissolution in neutral medium, the delay mechanism can be explained by Steps 1 and 2 only.

In the case of the dissolution of the tablet in acidic medium, one more step contributes to the delay of dissolution: the transformation of Mg-St to poorly soluble stearic acid on the tablet surface (Step 3), as confirmed by ATR-FTIR studies. Calculated in the same way as dissolution in pH 6.8 medium, the ratio of the initial dissolution rate of Mg-St(+) tablets to that of Mg-St(-) tablets, 0.47, indicates that 53% of the drug surface was covered by Mg-St and stearic acid in pH 1.2 medium. Compared to the decreased ratio in pH 6.8 medium, stearic acid may contribute to further decrease the effective surface area by 15%.

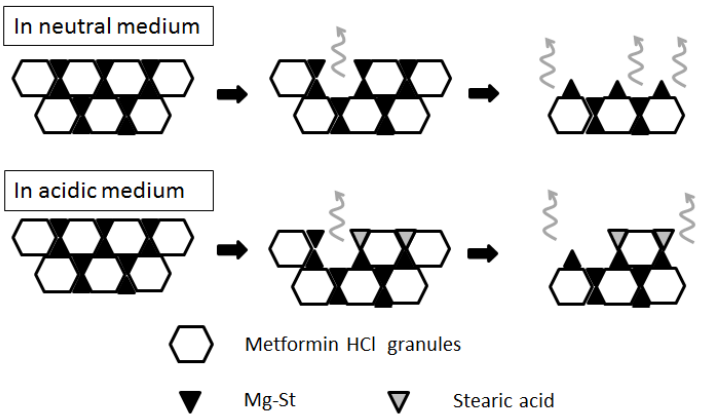

Figure 9 Illustration of delay mechanism of tablet dissolution by Mg-St; Step 1: Exposure of Mg-St on tablet surface (in acidic and neutral media); Step 2: Limitation of tablet dissolution by Mg-St dissolution (in acidic and neutral media); Step 3: Transformation of Mg-St to poorly-soluble stearic acid (only in acidic medium).

4. Conclusion

Mg-St is a well-known and commonly used lubricant for orally administered solid drug products. Therefore, there have been many studies that investigated the quantitative influence of Mg-St on rates of drug dissolution from tablets. These studies used tablets containing different amounts of Mg-St or tablets manufactured by different process parameters, which led to the investigation of potential lot-to-lot variation. The aim of this study was to investigate the mechanism of delay caused by Mg-St, and to determine the difference in the delay mechanisms in acidic and neutral media.

In this study, some spectroscopic techniques were applied to identify key factors and elucidate the mechanism of drug dissolution from metformin tablets containing Mg-St. The molecular-level change of Mg-St to stearic acid was detected by FTIR, and micro-level spatial distribution of Mg-St on the tablet surface was evaluated by SEM-EDS. As a result, the mechanism by which Mg-St inhibits the dissolution of tablets was proposed, and mechanism by which this inhibition is promoted in acidic pH environments was elucidated.

This research also proposed an evaluation approach using mutually complementary spectroscopic techniques that analyze the same question from different aspects would be effective. SEM-EDS and FTIR were used to investigate the properties of Mg-St. SEM-EDS detected Mg of Mg-St and FTIR detected the stearyl base of Mg-St, and the hypothesis that the amount of exposed Mg-St on the tablet surface increases after dissolution was suggested and supported by the findings obtained by both methods.

The model tablet used in this study was not the rapidly disintegrating type but a surface dissolution-type tablet. In the former type of tablet, the phenomenon reported in this study may not be observed, because the dissolution of Mg-St would not be a rate-limiting process for tablet dissolution. In the latter type of tablet, the same phenomenon as described in this study may occur. However, this also depends on the properties of the other components besides Mg-St. If the solubility of the drug is lower than that of Mg-St, its dissolution would become a rate-limiting process. In this study, the other components of the tablet (metformin HCl and povidone) were soluble, and their dissolution was not dependent on the pH of the medium. Therefore, the characteristics of Mg-St and the mechanism by which Mg-St causes the delay of tablet dissolution could be investigated clearly and separately from the other factors. The phenomenon observed in this study may be involved in the dissolution of other tablets in varying degrees, depending on the drug product.

Study 2: Non-destructive Prediction of Enteric Coating Layer Thickness and Drug Dissolution Rate by Near-infrared spectroscopy and X-ray computed tomography

1. Background

Enteric-coated products are intended to dissolve in the small intestine, not in the stomach, and represent one of the controlled-release products which require the proper control of *in vivo* dissolution. One commonly used enteric coating ingredient is pH-dependent polymers, which contain carboxylic acid groups. This coating remains undissolved in the low pH of the stomach and starts to dissolve slowly in the neutral pH of the small intestine. Thus, the pH-dependent dissolution property of the enteric-coated products depends on the solubility and pK_a of the drug and coating polymer, as well as the properties of the dissolution medium, such as pH and buffer capacity [2]. Additionally, it depends on the composition and thickness of the enteric coating layer [30].

Therefore, it is important for pharmaceutical manufacturing process to control the thickness of the enteric coating layer that determines the dissolution rate of the drug product to ensure a consistent product quality. There are many analytical techniques for investigation of the tablet surface, including the film coating layer. Microscopy, such as light microscopy and scanned electron microscopy (SEM), can be used to measure the layer thickness directly based on the expanded target image; however, cutting the target sample is necessary to expose the cross section of the coating layer, which leads to sample destruction. On the contrary, spectroscopy, such as attenuated total reflection-Fourier transform infrared (ATR-FTIR), near-infrared (NIR) [31–33], Raman [34,35], and terahertz spectroscopy [36], are non-destructive techniques. However, these techniques cannot directly measure the layer thickness, but can provide chemical quantitative information as absorption of light, from which the information of layer thickness can be derived depending on the optical path length. A correlation analysis between the obtained spectrum and the layer thickness allows the extraction of information and prediction of the layer thickness. NIR and Raman spectroscopy are often used as real-time monitoring techniques during the coating process because of their non-destructive nature and quick response [37–39]. Furthermore, combination of spectroscopic and imaging techniques can provide more detailed information. Previous studies showed that the spatial distribution data of the coating layer thickness can be obtained by NIR chemical imaging (CI) [32,40] and terahertz pulsed imaging (TPI) [38,41,42].

These non-destructive techniques enable the data acquisition of both coating layer thickness and drug dissolution rate for the same tablet by predictive measurement of the layer thickness followed by measurement of the dissolution rate of the same tablet. It is generally known that the coating layer thickness of tablets or pellets correlates with the drug dissolution rate [43,44]. Gendre et al. showed that the predicted layer thickness correlated with the dissolution rate of the product [45]. This

relation is more critical for enteric-coated tablets because of their thick coating layer and slow dissolution rate.

In this study, the correlation between enteric coating layer thickness and drug dissolution rate was investigated using several commercial aspirin enteric-coated tablets. Only a few researchers studied this relationship for enteric-coated tablets [46]. In addition to NIR, X-ray CT technique was adopted for non-destructive measurement of the coating layer thickness distribution. X-ray CT is a relatively new but a very strong tool for noninvasive investigation of the internal three-dimensional (3D) structures of various objects. It has been applied for monitoring of the dynamic changes inside tablets during the dissolution process [47,48] and evaluation of the coating layer thickness of particles [49,50].

2. Materials and methods

2.1 Materials

2.1.1. Materials

Two commercial enteric-coated aspirin 100 mg tablets were used, which were coded as product A and B. Only one lot for each product was used. The diameter was approximately 7 mm and the average weight was approximately 137 mg for both tablets. Aspirin core tablets of both products were prepared by removing the enteric coating layer.

The major components were acetylsalicylic acid (aspirin) and crystalline cellulose for aspirin core tablets, and methacrylic acid copolymer LD (L30D-55) and talc for enteric coating layer based on the information on the product documents.

To obtain reference NIR spectra of pure materials, aspirin, methacrylic acid copolymer LD (L30D-55), and talc were purchased from Nichi-iko pharmaceuticals (Toyama, Japan), Evonik industries (Essen, Germany), and Hayashi Chemicals (Tokyo, Japan), respectively.

2.1.2. Preparation of dissolution medium

For the dissolution tests, the 2nd fluid (pH 6.8) provided in the Japanese Pharmacopoeia 17th edition (JP17) was used, which was specified as the dissolution medium for release testing of many commercial aspirin tablets.

2.2 Methods

2.2.1. NIR measurement

A Fourier transform near-infrared spectroscopy (FT-NIR) apparatus (MPA, Bruker, Ettlingen, Germany) was used for surface measurement of the tablets. The scanning range was 12500 - 4000

cm^{-1}, resolution was 8 cm^{-1}, and scan integration number was 32. Using diffuse reflectance mode with an integration sphere, the NIR spectra of the tablet surface were obtained for both sides of each tablet as shown in Figure 10.

2.2.2. Measurement of enteric coating layer thickness

After NIR measurements, the tablet was cut vertically, as shown in Figure 10, and the cross section was observed using a digital microscope (VHX-100, Keyence, Osaka, Japan) attached with a zoom lens (VH-Z35, Keyence, Osaka, Japan) under low magnification of ×35. Along the outer coating layer of the cross section, the coating layer thickness at the tablet face and side regions was measured at more than 30 points at constant intervals.

The average coating layer thickness per each side of the tablet face was calculated using the thickness values at more than nine points, and represented the dependent variable for preparation of the NIR-based calibration model.

2.2.3. Development of a calibration model for coating layer thickness

For development of a calibration model using partial least squares (PLS) regression, OPUS 6.5 software (Bruker, Germany) was applied. For each product, data sets of 41 pairs of the NIR spectra and the corresponding enteric coating layer thickness values were prepared for PLS regression. The data sets included 40 pairs for each side of the 20 tablets and one pair of the NIR spectrum of aspirin core tablet without the coating layer. Test set validation was applied for the calibration model using 20 data pairs from 10 tablets as “Test” samples, and 21 pairs from the other 11 tablets, including one pair of aspirin core tablet, as “Calibration” samples.

2.2.4. Dissolution test

A dissolution test apparatus (NTR-6100A, Toyama Sangyo, Osaka, Japan) was used for the dissolution tests according to the paddle method described in JP17 using a rotation speed of 75 rpm. The test solution of 5 mL was sampled from each vessel at each time point, filtered through a 0.45-μm membrane filter and the drug concentration was determined by high-performance liquid chromatography (HPLC) analysis.

An appropriate HPLC apparatus with UV detection unit for the determination purpose was used. The determination method by HPLC was validated one, and the HPLC operating conditions were as follows: the analytical column was ODS (C18) column, and the mobile phase was a mixture of phosphate buffer (pH 6.8) and acetonitrile, UV detection wavelength was 267 nm, and the gradient program was applied for the analysis.

2.2.5. X-ray CT measurement for investigation of coating layer thickness

Each tablet was scanned by a microfocus x-ray CT system (inspeXio SMX-100CT, Shimadzu Corporation, Kyoto, Japan). The x-ray tube voltage and current were 60 kV and 40 μA, respectively. The area of 8.265 × 8.265 × 8.265 mm^3 for xyz dimension was scanned at about 16-μm resolution (512 × 512 × 512 voxels). The scanning conditions were a view number of 1200 and image average of 40 times. The measurement time was approximately 30 min for each tablet.

Based on the obtained 3D image of the absorption distribution, the film coating layer thickness was evaluated using VGStudioMAX (Volume Graphics, Heidelberg, Germany). The enteric coating layer is identified as a high absorption region; thus, the distribution of coating layer thickness was analyzed and visualized using the wall thickness analysis option.

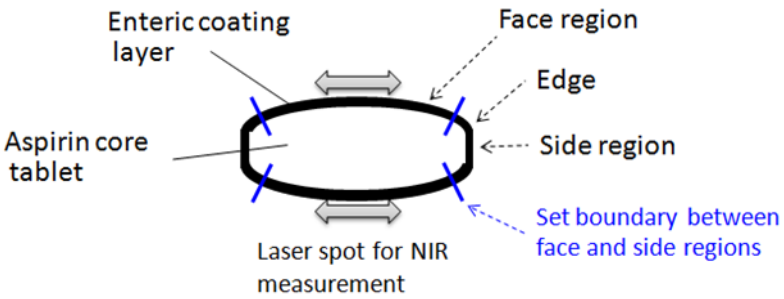

Figure 10　Illustration of the cross-section of aspirin enteric coated tablets. The area measured by NIR is presented by the arrow. The boundary is also presented which was set at 0.5 mm inside from the tablet edge to separate between the face and side regions for analysis of the coating layer thickness distribution.

3. Results and Discussion

3.1. Preparation of calibration models for evaluation of coating layer thickness of each product by NIR

Calibration models of enteric coating layer thickness were separately developed for product A and B because the coating layer composition of products A and B was supposed to be different looking into each product document. Based on the direct observation using the digital microscope, the layer thickness varied between 64 and 127 μm for product A, and between 71 and 133 μm for product B.

The major components of the enteric coating layer were methacrylic acid copolymer LD and talc. To determine the adequate wavenumber range in the NIR spectra to calibrate the coating layer thickness, the NIR spectra of the major components and core tablets were compared as shown in Figure 11. Because of the high aspirin content ratio, which was more than 73 % (100 mg aspirin in about 137 mg of tablet), the major component of the core tablet was aspirin; thus, the NIR spectra of the core tablets of products A and B corresponded to aspirin. A spectral difference between the coated tablet and core tablet was clearly observed at the regions at approximately 8500, 7200, 6000, and 4300 cm^{-1}. These differences should indicate an increase in the contribution of the coating materials, such as methacrylic acid copolymer LD and talc, as well as a decrease in the contribution of aspirin.

The characteristic absorption bands at 8480, 5960, 5800, 4430, and 4360 cm^{-1} were due to methacrylic acid copolymer, whereas the bands at 8840 and 6040 cm^{-1} were due to aspirin. The characteristic sharp absorption bands of talc were observed at 7190 and 4330 cm^{-1}. Additionally, the broad absorption bands of water were observed at the regions around 7000 and 5200 cm^{-1}. Therefore, spectral differences at approximately 8500, 7200, and 8800 cm^{-1} were attributed to the polymer, talc, and aspirin, respectively. Moreover, differences in the bands at approximately 6000 cm^{-1} were attributed to the polymer and aspirin. These regions should be included in the wavenumber range of the calibration model.

Thus, these wavenumber ranges were evaluated for the calibration model, (i) 12500-4000 cm^{-1} of the full range, (ii) 10000-4000 cm^{-1} without noisy range, and (iii) 10000-5500 cm^{-1} without water-derived absorption range. Additionally, as a preprocessing of NIR spectra, a standard normal variate (SNV), first derivative (FD, smoothing point: 17), or second derivative (SD, smoothing point: 17) was examined prior to PLS calibration. For product A, the root-mean-square error of prediction (RMSEP) of the validation results showed the smallest value (8.1 μm) and the coefficient correlation value was the highest when the PLS calibration was performed at the range of (i) 12500-4000 cm^{-1} with second derivative as a preprocessing and the number of explanatory variables (rank) was 2. The calibration curve and its regression spectrum are shown in Figure 12A. The curve indicated a good correlation (R^2 = 0.8683), and the regression spectrum appropriately detected the changes in the absorption bands attributed to aspirin, methacrylic acid copolymer, and talc. This

model was determined for the calibration of enteric coating layer thickness of product A.

Similarly, the calibration model for product B was optimized, as shown in Figure 12B. The parameters were determined based on the optimization study as follows: the range was 10000-4000 cm^{-1} with first derivative as the preprocessing and the number of explanatory variables (rank) was 3 (RMSEP = 5.21 μm). Good correlation was confirmed with R^2 = 0.8772. The regression spectrum suggested that this calibration model for product B was based on the chemical information of talc and aspirin. The resulting RMSEP value was sufficiently low owing to the coating roughness.

The regression spectra of the calibration models of products A and B were different. The model for product A was mainly contributed by the aspirin quantity decrease according to the increase in the coating layer thickness, whereas the contribution of aspirin quantity was not high for the model of product B, which was mainly contributed by the quantity of talc in enteric coating layer. The differences in the composition and density of the enteric coating layer between these products resulted in these different calibration models.

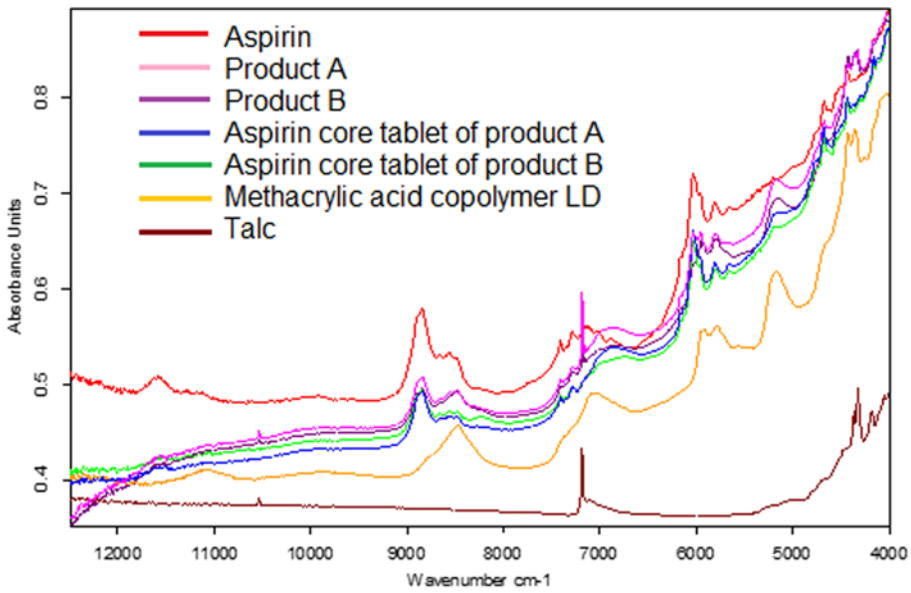

Figure 11 NIR spectra for products A and B and their components

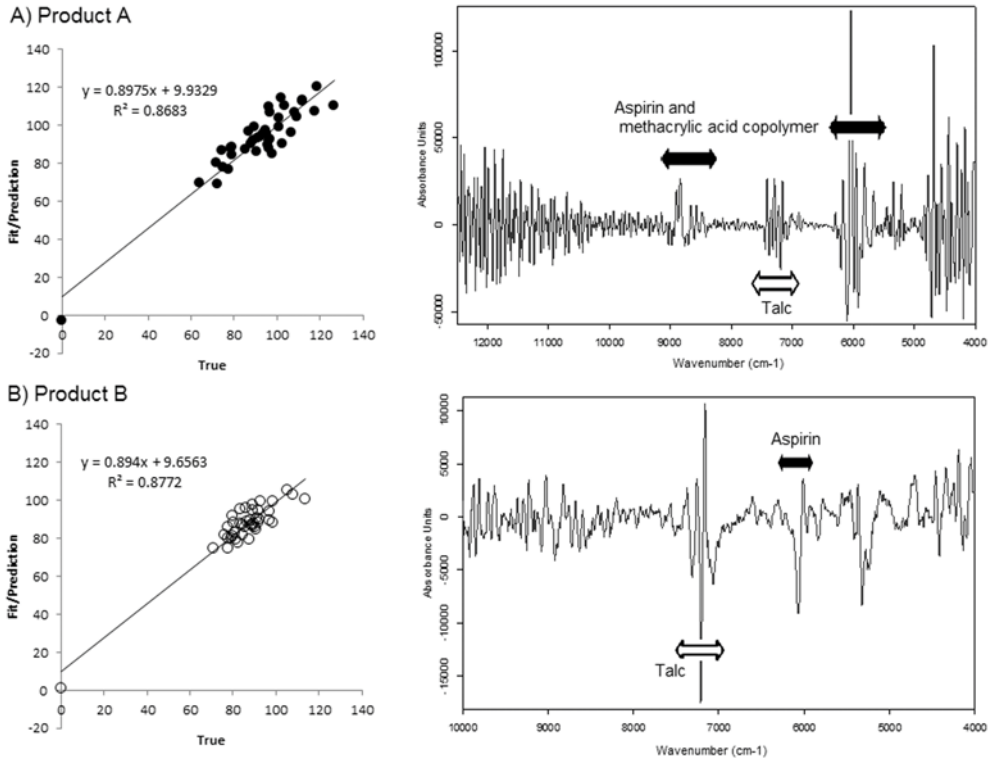

Figure 12　Calibration curve and regression spectrum of NIR calibration model for enteric coating layer thickness. A: product A (upper, 12500-4000 cm^{-1}, second derivative, rank 2); B: product B (lower, 10000-4000 cm^{-1}, first derivative, rank 3)

3.2. Prediction of the coating layer thickness and drug dissolution rates

To investigate the relation between the enteric coating layer thickness and drug dissolution rate, NIR spectra were collected for another twenty-four samples of product A and eighteen samples of product B, which were of the same lot as that of the tablets used for preparing the calibration models. The calibration models were used for predicting the coating layer thickness based on the collected spectra. The average layer thickness was calculated at both faces for each tablet. Following the NIR measurements, these tablets were applied to the dissolution testing, and their variable dissolution profiles are shown in Figure 13.

The % dissolved aspirin at 45 and 60 min was plotted as a function of the predicted coating layer thickness, as shown in Figure 14. The results of regression analysis are summarized in Table 2. It is known that the dissolution rate decreases with the increase in the coating layer thickness. This inverse relation was expectedly observed for product A at both time points as shown in Figure 14A: the correlation coefficient between dissolution% at 45 and 60 minutes and predicted thickness was -0.6575 and -0.6334, respectively, and the slope of both regression lines were statistically significant ($p<0.01$). Generally, the value of correlation coefficient less than -0.6 or larger than 0.6 indicates that those two values have the negative or positive correlation, respectively. Compared to the results for product B in Figure 14B where the correlation coefficient was 0.4001 and 0.2786 and the slope of regression lines was not statistically significant, it is concluded that the correlation was observed for product A. This negative correlation is consistent with the general knowledge about dissolution% and coating thickness.

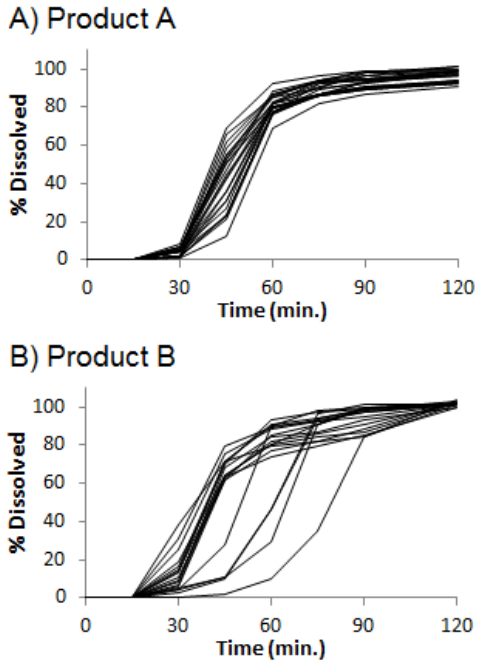

Figure 13 Individual dissolution profiles of products A and B

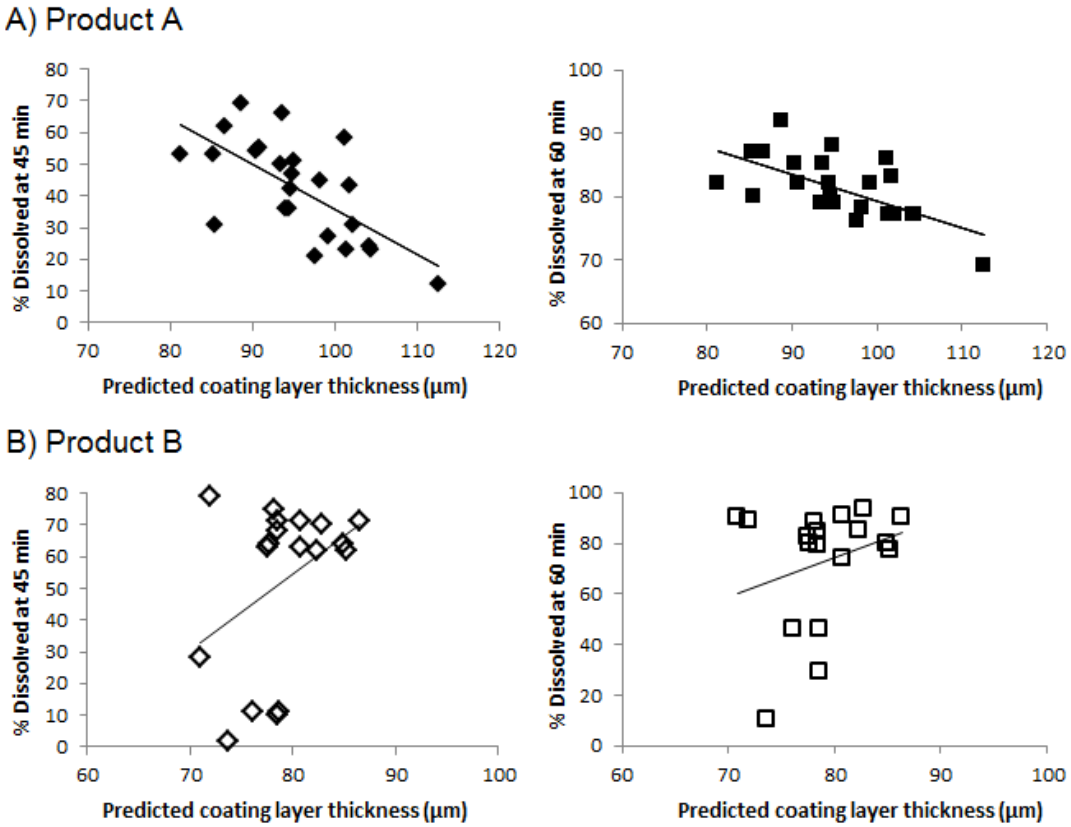

Figure 14 Relationship between % dissolved aspirin and predicted coating layer thickness for products A and B. The regression line is presented in each figure.

Table 2 Correlation between % dissolved and predicted coating layer thickness

	% dissolved at 45 min			% dissolved at 60 min vs.		
Sample	Slope	Intercept	Correlation Coefficient	Slope	Intercept	Correlation Coefficient
A	-1.412	177.1	-0.6575 (p=0.0005)	-0.4302	122.3	-0.6334 (p=0.0009)
B	2.438	-140.3	0.4001 (p=0.0999)	1.531	-48.15	0.2786 (p=0.2629)

3.3. Micro X-ray CT analysis of coating layer thickness distribution

Because the predicted coating layer thickness did not correlate with the drug dissolution rate, other factors might contribute to the drug dissolution of product B. Microscopic determination of the thickness distribution was necessary because NIR analysis could only provide the average macroscopic thickness of the target sample [32]. Although there are some techniques for microscopic measurements, including NIR-CI [32,40], Raman mapping [38], and TPI [41,42], X-ray CT was selected in this study because of its non-destructive nature and high spatial resolution. Additionally, X-ray CT directly provides the coating layer thickness; thus, it is an appropriate technique to determine the coating layer thickness and its distribution [50,51].

Three tablets for each of products A and B were scanned by X-ray CT system, and the 3D data of the X-ray absorption distribution was obtained. The extracted longitudinal section figures are shown in Figure 15. The absorption distribution is represented by a gray scale, where the color gradient from black to white corresponds to the gradient from low to high absorption. The enteric coating layer was clearly distinguished from the inner aspirin core tablet owing to the difference in the densities [52,53] and X-ray absorption properties of the materials. Thus, the outer region of high absorption area was determined to the enteric coating layer part. The distribution of the coating layer thickness was calculated for the whole tablet and mapped by color in Figure 16, where the color gradient from blue to red corresponds to the gradient from thin to thick layer.

As shown in Figure 16, the 3D images expressed green wholly and showed that the thickness was entirely constant within the tablet, including the faces, sides, and edges for any tablet of product A, which indicated intra-tablet homogeneity. On the contrary, two of three tablets of product B, shown in Figure 16 B-1 and B-3, expressed blue on the side regions in addition to green and showed an intra-tablet heterogeneous distribution of the coating layer thickness. The thickness at the sides and edges was less than that at the face regions. In order to evaluate the differences between the face and side regions quantitatively, the coating layer of each tablet was divided into two parts that represented the face and side regions based on the boundary shown in Figure 10. Then, the histograms of the layer thickness were constructed for each region of the tablets. All histograms of the six tablets are shown in Figure 17. Based on the histogram, the average thickness of each region of the tablets was summarized in Table 3. The average thickness was equal at the face and side regions for product A, whereas product B showed different average thickness at the face and side regions. In addition, the histogram of product A was symmetric, whereas that of product B was distorted and not symmetric, which indicated the heterogeneity of the coating layer thickness. It was suggested that the localized thin coating layer observed in tablets B-1 and B-3 might result in fast drug dissolution despite the equal thickness at the face regions to the other tablets.

These six tablets scanned by X-ray CT system were applied to the dissolution testing. Both products A and B showed similar dissolution patterns: (1) the horizontal crack first appeared on the

side region of the tablet, as shown in Figure 18, (2) the crack expanded to the whole side of the tablet, and (3) finally, the tablet disintegrated into two parts. The dissolved drug amounts were determined by HPLC, and the dissolution profile of each tablet is shown in Figure 18.

For product A, the crack appeared on the side region in the order of: A-3 (approximately 15 min), A-2 (approximately 17 min), and A-1 (approximately 19 min). Subsequently, the tablets disintegrated into two parts at approximately 32, 33, and 43 min for tablets A-2, A-3, and A-1, respectively. For product B, the crack appeared at 20, 22, and 25 min, and the tablet disintegrated at 35, 42, and 47 min for tablets B-3, B-2, and B-1, respectively. We observed that, by comparison of the observation with the drug dissolution profiles, the dissolution started at the time of cracking, and accelerated after the tablet disintegration. Crack formation is the critical step that determines the dissolution process; in addition, we suggest that the coating layer thickness at the side regions is the critical factor that affects crack formation. By comparison with the coating layer thickness at the side regions in Table 3, the perfect correlation between the average thin layer thickness at the side regions and the early crack formation was not observed. This would be due to the contribution of the micro spot of thinner layer thickness to the crack, however, it would be clear that thin layer thickness distribution at the side regions could contribute to the early crack formation.

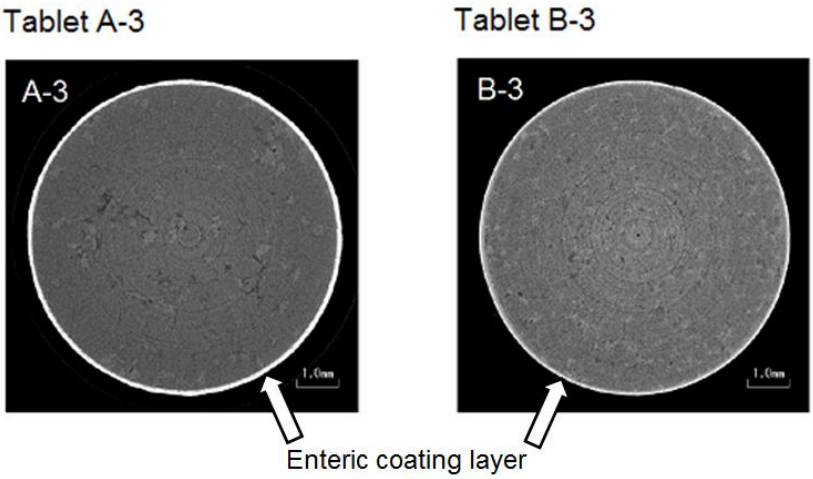

Figure 15　Longitudinal section images obtained using X-ray CT system for products A and B. The color gradient from black to white corresponds to the gradient from low to high absorption. The white part corresponds to the enteric coating layer part.

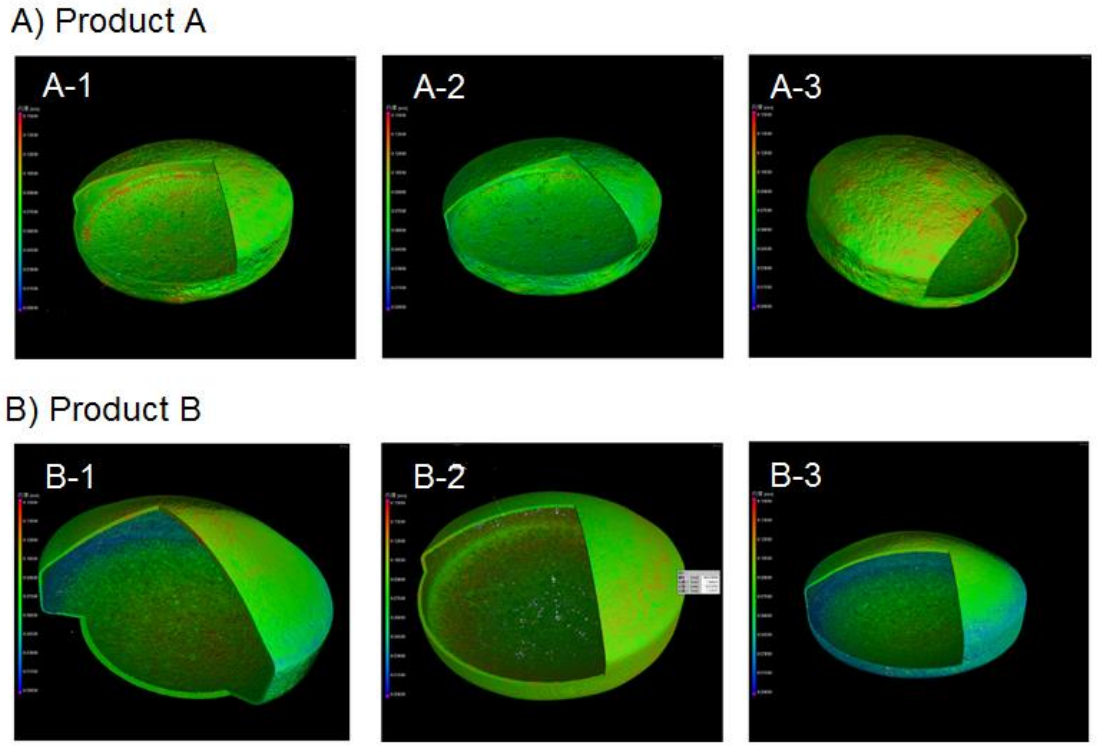

Figure 16 Color images of distribution of coating layer thickness of each six tablets. The color gradient from blue to red corresponds to the gradient from thin to thick layer thickness (0 - 150 μm).

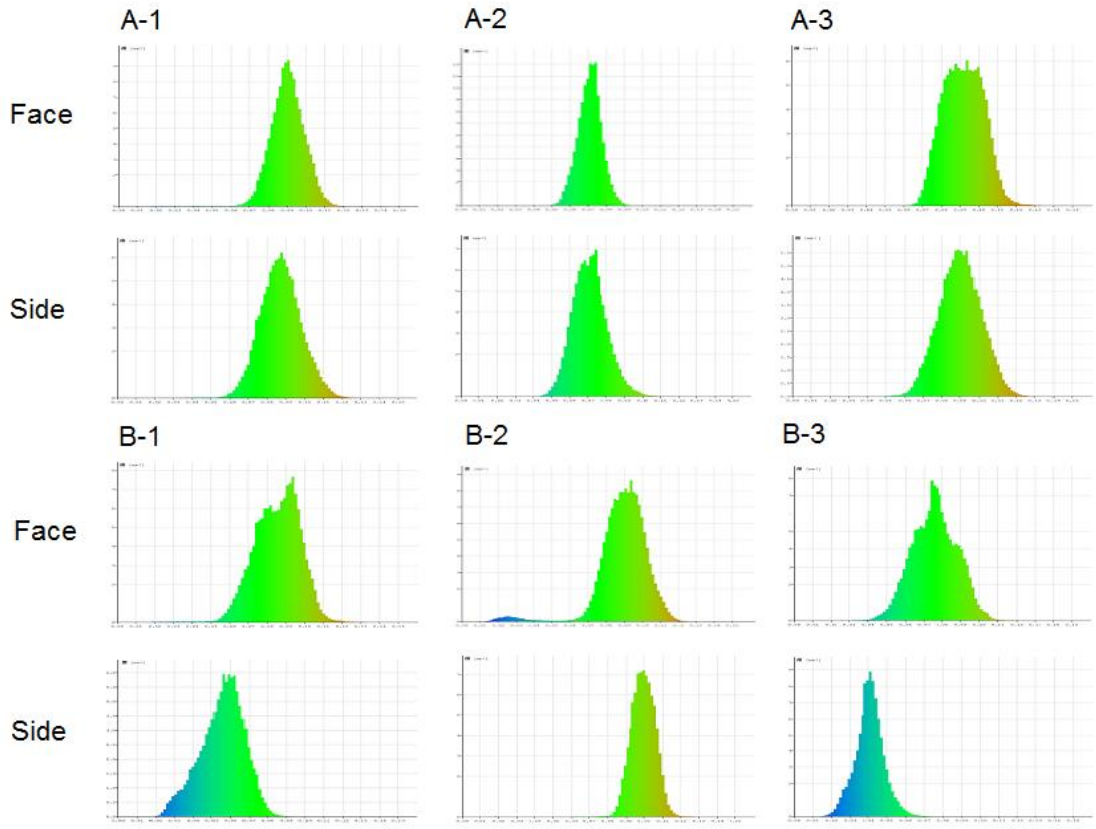

Figure 17　Separate histograms of coating layer thickness distribution for the face and side regions of the tablets. The horizontal axis represents the layer thickness from 0 to 150 μm.

Table 3　Coating layer thickness at the face and side regions of each tablet

Sample		**Thickness (μm)**		
		1	2	3
		Ave. ± SD	Ave. ± SD	Ave. ± SD
A	Face	90.3 ± 9.04	71.0 ± 6.50	91.8 ± 10.5
	Side	87.3 ± 10.9	71.1 ± 9.28	89.8 ± 11.2
B	Face	85.5 ± 12.1	89.4 ± 13.8	75.9 ± 12.1
	Side	55.7 ± 11.7	99.3 ± 6.87	40.6 ± 7.71

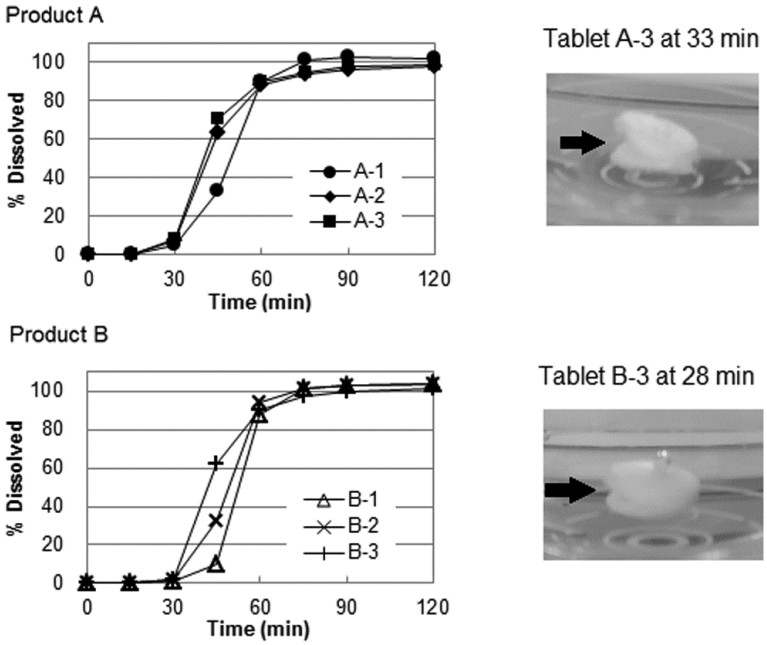

Figure 18 Individual dissolution profiles of the six tablets measured by X-ray CT system along with pictures of the crack on the tablet side

3.4. Prediction of dissolution rate by evaluation of coating layer thickness

The face regions of the tablet are usually measured in the off-line NIR analysis. For intra-tablet homogeneous products, the coating layer thickness at the face regions can represent the whole tablet. However, NIR analysis of the face regions is not applicable for intra-tablet heterogeneous products. Even if there is a difference in the coating layer thickness between the face and side regions, the consistent relationship between the thickness of the face and side regions may enable the prediction of the whole thickness and the dissolution rate. However, for product B, the heterogeneous relationship did not allow the prediction of the coating layer thickness and dissolution rate.

The development of manufacturing processes to ensure uniform film coating is complex and difficult [54]. Many factors can affect the roughness and homogeneity of the coating layer thickness, such as the composition of film coating suspension, types of enteric coating components [30], and coating process parameters [42,55]. Therefore, the difference in the roughness of the tablet surface, composition of enteric film layer, and coating process parameters might result in the intra-tablet heterogeneity and inter-tablet inconsistency for product B.

For evaluation and control of the dissolution property of tablets, it is important to understand the critical attributes that affect the drug dissolution rate. In this study, based on the X-ray CT measurements and observation of the tablet dissolution process, it was revealed that the critical attribute that affected the drug dissolution rate was the enteric coating layer thickness at the side regions of the tablets, which directly influenced the rate of tablet split and the subsequent drug dissolution. Although X-ray CT particularly provided information about the coating layer thickness distribution of the whole tablet including the side regions, it required much longer time than NIR. Actually, NIR is generally applied during the manufacturing process as a PAT tool owing to its flexible application and fast response. Moreover, NIR-based PAT was used in the coating process of tablets to predict the amount of the coating material required [31,37]. However, our results showed that not only the total coating amount but also the coating thickness of the side regions was critical attribute to control the quality of products. Thus, heterogeneous tablet coating leads to a disagreement between the coating amount and the coating thickness of the side regions, resulting in a disagreement between the coating amount and the drug dissolution rate. Therefore, to control drug dissolution rate, the coating amount and coating thickness of the face regions should be proportional to that of the side regions and to the dissolution rate. We suggest that homogeneous tablet coating is important to ensure the quality of the final products.

4. Conclusion

In this study, the molecular-level data derived from carboxylic group of aspirin and methacrylic acid copolymer and hydroxylic group of talc were obtained, and the enteric coating layer thickness

was determined by off-line NIR spectroscopic analysis. Additionally, the correlation between the thickness and drug dissolution rate was investigated to evaluate the predictability of the dissolution profile from the thickness. If the dissolution profile can be predicted based on the thickness, NIR monitoring of the coating process is useful to control the drug dissolution. However, the NIR-predicted thickness correlated with the dissolution rate only for tablets with homogeneous coating, and cannot be applied for the other tablets. The coating layer thickness must be homogeneous within each tablet, or the trend in distribution of the coating layer thickness must be consistent between the tablets to enable the prediction of drug dissolution rate. Many studies have shown that X-ray CT is a very useful tool to determine the distribution of the coating layer thickness of the whole tablet or particle [49,50]. In this study, the micro-level spatial data of X-ray absorption was obtained by X-ray CT, and the distribution of layer thickness for the whole tablet was calculated based on the data, which revealed the homogeneity and heterogeneity of the layer thickness distribution of the whole tablet, including the side regions, and enabled separate analysis of the divided parts. The application of micro- and macro-spectroscopic approaches to the enteric coating layer enabled identification of the factors determining the dissolution and revealed the correlation between enteric film-coating layer properties and dissolution of the tablet.

It is important to investigate and fully understand the processes that affect the final properties, such as drug dissolution, prior to the development of any prediction model. The prediction model is often based only on macroscopic measurements. However, microscopic measurements are recommended as a complementary technique. The combination approach using the macro- and micro-analysis is useful to understand the pharmaceutical properties, such as dissolution rate. We suggest that investigation of the pharmaceutical properties by several techniques enables the establishment of proper prediction models.

Acknowledgements

The authors want to thank Dr. Satoshi Iguchi from Shimadzu Corporation for his cooperation in the measurement and analysis using a micro-focus X-ray CT system and for his scientific discussions.

Overall Conclusion

In these two studies, some spectroscopic techniques were applied to identify key factors and elucidate the mechanism of drug dissolution from orally administered solid dosage forms by monitoring of the chemical change of the target material at molecular level and micro-level spatial analysis of targets. In the first study, the molecular-level change of Mg-St to stearic acid was detected by FTIR, and micro-level spatial distribution of Mg-St on the tablet surface was evaluated by SEM-EDS. As a result, the mechanism by which Mg-St inhibits the dissolution of tablets was proposed, and mechanism by which this inhibition is promoted in acidic pH environments was elucidated by spectroscopic approaches. In the second study, the molecular-level data derived from carboxylic group of aspirin and methacrylic acid copolymer and hydroxylic group of talc were obtained by NIRS, and utilized for calculation and prediction of the thickness of enteric-coating layer containing those materials. In addition, the micro-level spatial data of X-ray absorption was obtained by X-ray CT, and the distribution of layer thickness for the whole tablet was calculated based on the data. The application of micro- and macro-spectroscopic approaches to the enteric coating layer enabled identification of the factors determining the dissolution and revealed the correlation between enteric film-coating layer properties and dissolution of the tablet. As such, spectroscopic approaches for examination of the dissolution of orally administered drug products were established successfully through these studies.

The studies provided one important suggestion. Spectroscopic techniques cannot provide direct information; the spectrum data represent the light absorption or scattering attributable to factors such as the functional groups and arrangement of molecules, and does not present the target results directly. Therefore, it is important to apply more than one technique to demonstrate a hypothesis. In the first study, SEM-EDS and FTIR were used to investigate the properties of Mg-St. SEM-EDS detected Mg of Mg-St and FTIR detected the stearyl base of Mg-St, and the hypothesis that the amount of exposed Mg-St on the tablet surface increases after dissolution was suggested and supported by the findings obtained by both methods. This research proposed an evaluation approach using mutually complementary spectroscopic techniques that analyze the same question from different aspects would be effective.

The results of the second study provide another approach using mutually complementary techniques. A macroscopic technique like NIRS and a microscopic technique like X-ray CT each have its unique advantages and disadvantages. Generally, macroscopic techniques provide results quickly, but the resolution of the results may be not high. In contrast, microscopic techniques can provide detailed data, but they require more time to measure and analyze the results. The balance between the operation time and the resolution of the data obtained should be considered depending on the purpose. The research results demonstrated the importance of a microscopic evaluation before

a macroscopic evaluation, e.g., by investigation of layer thickness distribution by X-ray CT before monitoring of total coating amount by NIRS in this case. Here, it was important to apply both macro- and microscopic techniques, which are also considered mutually complementary, to the same target.

Spectroscopic techniques offer such challenges; however, they are useful and appropriate tools for investigation of the dissolution properties and mechanisms of drug products due to their ability to perform nondestructive prediction of physicochemical properties or real-time monitoring of dynamic physicochemical properties. The important point is to apply spectroscopic techniques with a full understanding of their characteristics and limitations.

While these two studies yielded analytical knowledge and established the techniques, they also provided some suggestions for product quality and pharmaceutical product development. The results of the first study indicated the potentially different behavior of Mg-St in acidic and neutral pH environments. This might suggest a change from Mg-St to another lubricant, e.g., a lubricant showing constant solubility in the physiological pH range or a more soluble lubricants [5]. When testing a new lubricant, the approach employed to evaluate the behavior of Mg-St in this study may be used to evaluate the new lubricant. The results of the second study showed the importance of thickness homogeneity of the film coating layer. Even when the film coating process is controlled and monitored by PAT tools like NIR, the homogeneity of the film layer thickness should be ensured beforehand. It is generally known that the PK profiles of aspirin enteric-coated tablets show much variation, thus the enteric-coating layer thickness should be kept consistent between tablets with intra-tablet homogeneity to avoid the dissolution variation between tablets that potentially contribute to the PK variation. Similarly, when the evaluation procedure is established using noninvasive spectroscopic techniques and the key factors determining dissolution are identified, provision of feedback to pharmaceutical product quality becomes possible.

In conclusion, some spectroscopic approaches were established for identification of key factors and elucidation of the mechanism of drug dissolution from orally administered solid dosage forms such as IR tablets and enteric-coated tablets. These approaches could be applied for other types of drug products, and could contribute to pharmaceutical product development, which is becoming increasingly complex. In addition, these results may contribute to advancement of the field of formulation development.

References

[1] G.L. Amidon, H. Lennernäs, V.P. Shah, J.R. Crison, A theoretical basis for a biopharmaceutic drug classification: the correlation of in vitro drug product dissolution and in vivo bioavailability., Pharm. Res. 12 (1995) 413–420. doi:10.1023/A:1016212804288.

[2] S.S. Ozturk, B.O. Palsson, B. Donohoe, J.B. Dressman, Kinetics of Release from Enteric-Coated Tablets, Pharm. Res. An Off. J. Am. Assoc. Pharm. Sci. 5 (1988) 550–565. doi:10.1023/A:1015937912504.

[3] V.S. Dave, H.I. Shahin, S.R. Youngren-Ortiz, M.B. Chougule, R. V. Haware, Emerging technologies for the non-invasive characterization of physical-mechanical properties of tablets, Int. J. Pharm. 532 (2017) 299–312. doi:10.1016/j.ijpharm.2017.09.009.

[4] K. Korasa, F. Vrečer, Overview of PAT process analysers applicable in monitoring of film coating unit operations for manufacturing of solid oral dosage forms, Eur. J. Pharm. Sci. 111 (2018) 278–292. doi:10.1016/j.ejps.2017.10.010.

[5] J. Wang, H. Wen, D. Desai, Lubrication in tablet formulations, Eur. J. Pharm. Biopharm. 75 (2010) 1–15. doi:10.1016/j.ejpb.2010.01.007.

[6] G. Levy, R.H. Gumtow, Effect of certain tablet formulation factors on dissolution rate of the active ingredient III. Tablet lubricants, J. Pharm. Sci. 52 (1963) 1139–1144. doi:10.1002/jps.2600521209.

[7] K.D. Ertel, J.T. Carstensen, An examination of the physical properties of pure magnesium stearate, Int. J. Pharm. 42 (1988) 171–180. doi:10.1016/0378-5173(88)90173-1.

[8] S.H.W.P. Okoye, Lubrication of Direct-Compressible Blends with Magnesium Stearate Monohydrate and Dihydrate, Pharm. Technol. (2007) 116–129. http://www.pharmtech.com/lubrication-direct-compressible-blends-magnesium-stearate-monohydrate-and-dihydrate.

[9] L. Roblot-Treupel, F. Puisieux, Distribution of magnesium stearate on the surface of lubricated particles, Int. J. Pharm. 31 (1986) 131–136. doi:10.1016/0378-5173(86)90222-X.

[10] K.T. Mitrevej, L.L. Augsburger, Adhesion of tablets in a rotary tablet press II. Effects of blending time, running time, and lubricant concentration, Drug Dev. Ind. Pharm. 8 (1982) 237–282. doi:10.3109/03639048209022100.

[11] M. Otsuka, I. Yamane, Y. Matsuda, Effects of lubricant mixing on compression properties of various kinds of direct compression excipients and physical properties of the tablets, Adv. Powder Technol. 15 (2004) 477–493. doi:10.1163/1568552041270563.

[12] M. Otsuka, J.I. Gao, Y. Matsuda, Effects of Mixer and Mixing Time on the Pharmaceutical Properties of Theophylline Tablets Containing Various Kinds of Lactose as Diluents, Drug Dev. Ind. Pharm. 19 (1993) 333–348. doi:10.3109/03639049309038771.

[13] J.G. Van der Watt, M.M. de Villiers, The effect of V-mixer scale-up on the mixing of magnesium stearate with direct compression microcrystalline cellulose, Eur. J. Pharm. Biopharm. 43 (1997) 91–94. doi:10.1016/S0939-6411(96)00005-7.

[14] J.-I. Kikuta, N. Kitamori, Effect of Mixing Time on the Lubricating Properties of Magnesium Stearate and the Final Characteristics of the Compressed Tablets, Drug Dev. Ind. Pharm. 20 (1994) 343–355. doi:10.3109/03639049409050187.

[15] K.S. Murthy, J.C. Samyn, Effect of shear mixing on in vitro drug release of capsule formulations containing lubricants, J. Pharm. Sci. 66 (1977) 1215–1219. doi:10.1002/jps.2600660903.

[16] T. Uchimoto, Y. Iwao, K. Takahashi, S. Tanaka, Y. Agata, T. Iwamura, A. Miyagishima, S. Itai, A comparative study of glycerin fatty acid ester and magnesium stearate on the dissolution of acetaminophen tablets using the analysis of available surface area, Eur. J. Pharm. Biopharm. 78 (2011) 492–498. doi:10.1016/j.ejpb.2011.01.014.

[17] T. Uğurlu, M. Turkoğlu, Hexagonal boron nitride as a tablet lubricant and a comparison with conventional lubricants., Int. J. Pharm. 353 (2008) 45–51. doi:10.1016/j.ijpharm.2007.11.018.

[18] F. Ebba, P. Piccerelle, P. Prinderre, D. Opota, J. Joachim, Stress relaxation studies of granules as a function of different lubricants, Eur. J. Pharm. Biopharm. 52 (2001) 211–220. doi:10.1016/S0939-6411(01)00171-0.

[19] M.S.H. Hussain, P. York, P. Timmins, Effect of commercial and high purity magnesium stearates on in-vitro dissolution of paracetamol DC tablets, Int. J. Pharm. 78 (1992) 203–207. doi:10.1016/0378-5173(92)90372-9.

[20] D.S. Desai, B.A. Rubitski, S.A. Varia, A.W. Newman, Physical interactions of magnesium stearate with starch-derived disintegrants and their effects on capsule and tablet dissolution, Int. J. Pharm. 91 (1993) 217–226. doi:10.1016/0378-5173(93)90341-C.

[21] K. Sekiguchi, K. Shirotani, M. Kanke, Dissolution Behavior of Solid Drugs. IV. Determination of Effective Surface Areas of Pharmaceutical Powders by Dissolution Rate Measurements, Pharm. Soc. Japan. 95 (1975) 195–203. http://ci.nii.ac.jp/naid/110003652031/.

[22] A. a Noyes, W.R. Whitney, The Rate of Solution of Solid Substances in Their Own Solutions, J. Am. Chem. Soc. 19 (1897) 930–934. doi:10.1021/ja02086a003.

[23] EMEA, Guideline on the investigation of bioequivalence, EMEA, n.d. CPMP/EWP/QWP/1401/98 Rev. 1/ Corr.

[24] C.L. Cheng, L.X. Yu, H.L. Lee, C.Y. Yang, C.S. Lue, C.H. Chou, Biowaiver extension potential to BCS Class III high solubility-low permeability drugs: Bridging evidence for metformin immediate-release tablet, Eur. J. Pharm. Sci. 22 (2004) 297–304.

doi:10.1016/j.ejps.2004.03.016.

[25] A.E. Bretnall, G.S. Clarke, Metformin Hydrochloride, Anal. Profiles Drug Subst. Excipients. 25 (1998) 243–293. doi:10.1016/S0099-5428(08)60757-1.

[26] R. Paus, E. Hart, Y. Ji, A novel approach for predicting the dissolution profiles of pharmaceutical tablets, Eur. J. Pharm. Biopharm. 96 (2015) 53–64. doi:10.1016/j.ejpb.2015.06.029.

[27] M.S.H. Hussain, P. York, P. Timmins, A study of the formation of magnesium stearate film on sodium chloride using energy-dispersive X-ray analysis, Int. J. Pharm. 42 (1988) 89–95. doi:10.1016/0378-5173(88)90164-0.

[28] E. Fukui, N. Miyamura, M. Kobayashi, Effect of magnesium stearate or calcium stearate as additives on dissolution profiles of diltiazem hydrochloride from press-coated tablets with hydroxypropylmethylcellulose acetate succinate in the outer shell, Int. J. Pharm. 216 (2001) 137–146. doi:10.1016/S0378-5173(01)00580-4.

[29] S.B. Marwaha, M.H. Rubinstein, Structure-lubricity evaluation of magnesium stearate, Int. J. Pharm. 43 (1988) 249–255. doi:10.1016/0378-5173(88)90281-5.

[30] R. Albanez, M. Nitz, O.P. Taranto, Influence of the type of enteric coating suspension, coating layer and process conditions on dissolution profile and stability of coated pellets of diclofenac sodium, Powder Technol. 269 (2015) 185–192. doi:10.1016/j.powtec.2014.09.016.

[31] C. Gendre, M. Genty, M. Boiret, M. Julien, L. Meunier, O. Lecoq, M. Baron, P. Chaminade, J.M. Péan, Development of a Process Analytical Technology (PAT) for in-line monitoring of film thickness and mass of coating materials during a pan coating operation, Eur. J. Pharm. Sci. 43 (2011) 244–250. doi:10.1016/j.ejps.2011.04.017.

[32] C. V. Möltgen, T. Puchert, J.C. Menezes, D. Lochmann, G. Reich, A novel in-line NIR spectroscopy application for the monitoring of tablet film coating in an industrial scale process, Talanta. 92 (2012) 26–37. doi:10.1016/j.talanta.2011.12.034.

[33] J.D. Kirsch, J.K. Drennen, Near-infrared spectroscopic monitoring of the film coating process., Pharm. Res. 13 (1996) 234–237. doi:10.1023/A:1016039014090.

[34] J.F. Kauffman, M. Dellibovi, C.R. Cunningham, Raman spectroscopy of coated pharmaceutical tablets and physical models for multivariate calibration to tablet coating thickness, J. Pharm. Biomed. Anal. 43 (2007) 39–48. doi:10.1016/j.jpba.2006.06.017.

[35] S. Romero-Torres, J.D. Pérez-Ramos, K.R. Morris, E.R. Grant, Raman spectroscopic measurement of tablet-to-tablet coating variability, J. Pharm. Biomed. Anal. 38 (2005) 270–274. doi:10.1016/j.jpba.2005.01.007.

[36] J.A. Zeitler, Pharmaceutical Terahertz Spectroscopy and Imaging, in: A. Müllertz, Y. Perrie, T. Rades (Eds.), Anal. Tech. Pharm. Sci., Springer New York, New York, NY, 2016: pp.

171–222. doi:10.1007/978-1-4939-4029-5_5.

[37] J.D. Pérez-Ramos, W.P. Findlay, G. Peck, K.R. Morris, Quantitative analysis of film coating in a pan coater based on in-line sensor measurements., AAPS PharmSciTech. 6 (2005) E127–E136. doi:10.1208/pt060120.

[38] J. Müller, D. Brock, K. Knop, J. Axel Zeitler, P. Kleinebudde, Prediction of dissolution time and coating thickness of sustained release formulations using Raman spectroscopy and terahertz pulsed imaging, Eur. J. Pharm. Biopharm. 80 (2012) 690–697. doi:10.1016/j.ejpb.2011.12.003.

[39] J.J. Moes, M.M. Ruijken, E. Gout, H.W. Frijlink, M.I. Ugwoke, Application of process analytical technology in tablet process development using NIR spectroscopy: Blend uniformity, content uniformity and coating thickness measurements, Int. J. Pharm. 357 (2008) 108–118. doi:10.1016/j.ijpharm.2008.01.062.

[40] L. Maurer, H. Leuenberger, Terahertz pulsed imaging and near infrared imaging to monitor the coating process of pharmaceutical tablets, Int. J. Pharm. 370 (2009) 8–16. doi:10.1016/j.ijpharm.2008.11.011.

[41] L. Ho, R. Müller, K.C. Gordon, P. Kleinebudde, M. Pepper, T. Rades, Y. Shen, P.F. Taday, J.A. Zeitler, Applications of terahertz pulsed imaging to sustained-release tablet film coating quality assessment and dissolution performance, J. Control. Release. 127 (2008) 79–87. doi:10.1016/j.jconrel.2008.01.002.

[42] M. Niwa, Y. Hiraishi, K. Terada, Evaluation of Coating Properties of Enteric-Coated Tablets Using Terahertz Pulsed Imaging, Pharm. Res. (2014) 1–12. doi:10.1007/s11095-014-1314-6.

[43] J.D. Kirsch, J.K. Drennen, Determination of film-coated tablet parameters by near-infrared spectroscopy, J. Pharm. Biomed. Anal. 13 (1995) 1273–1281. doi:10.1016/0731-7085(95)01562-Y.

[44] P.M. Satturwar, P.M. Mandaogade, S. V Fulzele, G.N. Darwhekar, S.B. Joshi, a K. Dorle, Synthesis and evaluation of rosin-based polymers as film coating materials., Drug Dev. Ind. Pharm. 28 (2002) 381–7. doi:10.1081/DDC-120002999.

[45] C. Gendre, M. Boiret, M. Genty, P. Chaminade, J.M. Pean, Real-time predictions of drug release and end point detection of a coating operation by in-line near infrared measurements, Int. J. Pharm. 421 (2011) 237–243. doi:10.1016/j.ijpharm.2011.09.036.

[46] J.A. Spencer, Z. Gao, T. Moore, L.F. Buhse, P.F. Taday, D.A. Newnham, Y. Shen, A. Portieri, A. Husain, Delayed release tablet dissolution related to coating thickness by terahertz pulsed image mapping., J. Pharm. Sci. 97 (2008) 1543–50. doi:10.1002/jps.21051.

[47] M. Otsuka, K. Ibe, Y. Tokudome, H. Ohshima, Nano- and macro-geometrical structural change of caffeine and theophylline anhydrate tablets during hydration process by using X-ray computed tomography, Colloids Surfaces B Biointerfaces. 73 (2009) 351–359.

doi:10.1016/j.colsurfb.2009.06.002.

[48] H. Li, X. Yin, J. Ji, L. Sun, Q. Shao, P. York, T. Xiao, Y. He, J. Zhang, Microstructural investigation to the controlled release kinetics of monolith osmotic pump tablets via synchrotron radiation X-ray microtomography, Int. J. Pharm. 427 (2012) 270–275. doi:10.1016/j.ijpharm.2012.02.017.

[49] G. Perfetti, E. Van De Casteele, B. Rieger, W.J. Wildeboer, G.M.H. Meesters, X-ray micro tomography and image analysis as complementary methods for morphological characterization and coating thickness measurement of coated particles, Adv. Powder Technol. 21 (2010) 663–675. doi:10.1016/j.apt.2010.08.002.

[50] F. Sondej, A. Bück, K. Koslowsky, P. Bachmann, M. Jacob, E. Tsotsas, Investigation of coating layer morphology by micro-computed X-ray tomography, Powder Technol. 273 (2015) 165–175. doi:10.1016/j.powtec.2014.12.050.

[51] J.A. Zeitler, L.F. Gladden, In-vitro tomography and non-destructive imaging at depth of pharmaceutical solid dosage forms, Eur. J. Pharm. Biopharm. 71 (2009) 2–22. doi:10.1016/j.ejpb.2008.08.012.

[52] D.H. Phillips, J.J. Lannutti, Measuring physical density with X-ray computed tomography, NDT E Int. 30 (1997) 339–350. doi:http://dx.doi.org/10.1016/S0963-8695(97)00020-0.

[53] I.C. Sinka, S.F. Burch, J.H. Tweed, J.C. Cunningham, Measurement of density variations in tablets using X-ray computed tomography, Int. J. Pharm. 271 (2004) 215–224. doi:10.1016/j.ijpharm.2003.11.022.

[54] R. Albanez, M. Nitz, O.P. Taranto, Enteric coating process of diclofenac sodium pellets in a fluid bed coater with a wurster insert: Influence of process variables on coating performance and release profile, Adv. Powder Technol. 24 (2013) 659–666. doi:10.1016/j.apt.2012.12.003.

[55] G. Perfetti, T. Alphazan, P. Van Hee, W.J. Wildeboer, G.M.H. Meesters, Relation between surface roughness of free films and process parameters in spray coating, Eur. J. Pharm. Sci. 42 (2011) 262–272. doi:10.1016/j.ejps.2010.12.001.

List of Publications

This dissertation is based on the following publications.

Aoi Ariyasu, Yusuke Hattori, and Makoto Otsuka. Delay effect of magnesium stearate on tablet dissolution in acidic medium. *Int. J. Pharm.* 2016; 511: 757–764.

Aoi Ariyasu, Yusuke Hattori, and Makoto Otsuka. Non-destructive prediction of enteric coating layer thickness and drug dissolution rate by near-infrared spectroscopy and X-ray computed tomography. *Int. J. Pharm.* 2017; 525: 282–290.

Acknowledgement

The studies in the present thesis were carried out under the direction of Professor Dr. Makoto Otsuka at Graduate School of Pharmaceutical Sciences, Musashino University, Japan. The author wishes to express her sincere gratitude to Professor Dr. Makoto Otsuka for his encouragement and valuable advice all through these studies.

The author is sincerely grateful to Dr. Yusuke Hattori and all members in Laboratory of Pharmaceutical Technology, Graduate School of Pharmaceutical Sciences, Musashino University, Japan for their encouragement, supports and helpful suggestions.